1996

Skelton model for the body structure of a passenger car

Young-Woo Lee
Lehigh University

Lee, Young-Woo

Skeleton Model for the Body Structure of a Passenger Car

June 2, 1996

Skeleton Model for the Body Structure of a Passenger Car

by

Young-Woo Lee

A Thesis

Presented to the Graduate and Research Committee

of Lehigh University

in Candidacy for the Degree of

Master of Science

in

Department of

Mechanical Engineering

Lehigh University

Bethlehem, Pennsylvania

May 1996

This thesis is accepted and approved in partial fulfillment of the requirement for the Master of Science.

May 3, 1996

date

Professor Arturs Kalnins

Thesis Advisor

Professor Robert P. Wei

Chairman of Department

Acknowledgment

I would like to express my sincere thanks to my advisor, Professor Arturs Kalnins, for his instruction and aid through this thesis. Also thanks to Hyundai Motor Company which has supported me for this opportunity and Korean Students in Lehigh University.

Above all, I greatly appreciate my lovely wife for her continuous assistance in my study, and especially, I willingly attribute this glory to my mother in Korea who might be so solitary and lonesome after sending her youngest son to study abroad.

TABLE OF CONTENTS

List of Figures

List of Symbols

K : Stiffness Matrix

C : Damping Matrix

M : Mass Matrix

$\ddot{U}$: Acceleration Vector

$\dot{U}$: Velocity Vector

U : Displacement Vector

F : External Force Vector

EI : Static Bending Stiffness

GJ : Static Torsional Rigidity

L : Wheel Base

W : Wheel Tread

θ : Twisting Angle

ω : Natural Frequency

ϕ : Eigenvector

λ : Eigenvalue

I : Identity Matrix

I_{yy}, I_{zz} : Moments of Inertia

J : Torsional Constant

D : Flexural Rigidity of the Plate

E : Young's Modulus

υ : Poisson's Ratio

t : Thickness of Plates

M_{mm} : Master Partitioning Mass Matrix

M_{ss} : Slave Partitioning Mass Matrix

K_{mm} : Master Partitioning Stiffness Matrix

K_{ss} : Slave Partitioning Stiffness Matrix

U_m : Master Partitioning Displacement Vector

U_s : Slave Partitioning Displacement Vector

K^{-1} : Inverse Stiffness Matrix

ϕ^T : Transposed Matrix of ϕ

a : Distance between Front Axle and Location of the Applied Load

b : Distance between Rear Axle and Location of the Applied Load

x : Location of Maximum Deflection

y : Maximum Vertical Deflection

Abstract

Finite element analysis is by now widespread in the automotive industry. For example, the finite-element detailed model of the body structure for passenger cars can be defined as a tool that can predict its performance. But such a detailed model is too complicated for the initial design concept stage. For this reason, a simplified model is developed.

In this thesis, a skeleton model is constructed and represented by only beam and spring elements. From this model, several kinds of analysis results are derived for static bending and torsional stiffness as well as natural frequencies and their corresponding mode shapes for body structure of a passenger car, by using commercial software I-DEAS. Moreover, upon comparing these analytic results with test results, it is shown that this skeleton model is a reasonable and reliable approximation of the actual body structure. Modifications are described that can improve the analytic results.

Chapter 1

INTRODUCTION

In the case of a complicated vehicle, it is assembled by tens of thousands parts and the most significant part of them is its body structure. Therefore, it is very important to know how to design body structure. Many body-structure designers try to maximize the efficiency of design in the automotive industry. There are several ways to pursue that, but there are both merits and demerits from the standpoint of their objectives and methodology. Among them, it is necessary to predict the performance of the body structure in the early design stage.

For these reasons, many car designers have been working to develop those techniques. There is a necessity to build a skeleton model of body structure that can predict and evaluate its performance. Therefore, it is desired to study how to construct the reasonable and reliable skeleton model for the body structure. If this development is successful, it will be very helpful to the many body- structure designers.

1.1 Objectives, Motivations and Scope

As a way to evaluate the performance of the body structure for passenger cars analytically, the approach of finite element analysis is widely well-known in the field of computer aided engineering[1]. But currently, in the case of previous detailed finite element model, it has many elements to represent the real parts and needs much CPU

time to analyze this model. Moreover, if design specifications are needed to change to improve its performance, there might be many constraints regarding to the relating parts. This is because the analysis for the detailed model can be carried out only after the detailed drawings have been prepared. From these reasons, a more simplified finite element model such as a skeleton model represented by only beam and spring elements is needed.

The purpose of this thesis is to develop a skeleton model of a passenger car that is able to predict and estimate its performance in the early design stage through computer simulation that is based on the finite element analysis. Besides of that, in this thesis, comparisons of the results between analysis and test is performed to verify the appropriateness of this approach. Furthermore, it is possible to apply various analytic approaches by using this skeleton model in the future.

1.2 Background

Design of the body structure for passenger cars accompanies many difficulties to optimize its performance, because of the complexity of body structure, the variety of the function needed by the customers, reduction of the product's life cycle, and the trend of light-weight products[2].

To solve these problems, engineers have depended mainly on the method of tests. Of course, through the tests, it is necessary to go through many trials and errors to improve the models' performance, which may be expensive. Also, the tests can be carried out only after making prototype cars, which may result in production delays.

Therefore, it is desirable to develop a skeleton model by finite element analysis. Moreover, in the case of finite element analysis, once a FE model is constructed, various analytic simulations can be done[3]. The importance of this technique is increasing in the automotive industry day after day.

Chapter 2

CONSTRUCTION OF SKELETON MODEL

2.1 Introduction

The body structure of passenger cars is assembled from substructures, which consist of several panel parts and are fabricated by spot welding. These substructures are classified into two groups. One of them consists of members and pillars that are of the closed-section type, or box-type, substructures, and the other consists of panel parts, such as a roof panel, center floor panel, rear floor panel etc.. The stiffness of the body structure for passenger cars depends mainly on the substructures of members.

In this thesis, the body structure is considered as consisting of closed-section type members and open-section type panels, and these substructures are represented by one-dimensional beam or rod elements. By doing so, the model size can be greatly reduced in comparison to a finely meshed model that is generated by shell elements. On the other hand, if the body structure is expressed just as beam elements in the skeleton model, there may be some problems around joint parts, where members are interconnected. This is because, in real structure, those joint parts are designed very smoothly. For this reason, these joint parts may be too stiff in the skeleton model. Therefore, to compensate for these problems, flexible joints that are represented by beam and spring elements are applied in the skeleton model, and by doing so, this

finite-element skeleton model can be expected to model more closely the real body structure.

2.2 Modeling of Closed-Section Type Parts

2.2.1 Typical Sections of the Body Structure

The typical sections of the body structure are decided by considering several factors, such as a package layout, stiffness requirements, exterior styling, and interior capacity in the early design stage. But one of the most basic requirements that should be satisfied in new car development is the stiffness and strength of the body structure. Therefore, it is very important to know how to set up those typical sections initially. Configurations and geometry of these typical sections for the body structure are shown in Appendix A of this thesis. In general, section properties of the body structure are chiefly depended on both the sizes of cross sectional areas and the thicknesses of the parts. Of course, the larger are the typical sections, the more important are the section properties, such as moments of inertia, torsional constants, etc.. So, most of designers try to set up those typical sections as large as possible, and they have to be considered very carefully from the viewpoint of their great contributions to the stiffness distribution of the body structure.

2.2.2 Calculation of Section Properties

From the typical sections of the body structure, the section properties such as a cross-sectional area, moments of inertia, torsional constant, eccentricity, and the offset

of beam elements etc. can be obtained. There are many methods in calculating those properties. In the case of simple sections, they can be calculated manually. But, generally, the typical sections of the body structure are very complex and have arbitrary shapes, and it is very difficult to calculate their properties manually. So, instead of the manual method, special software is used to calculate those properties. In this thesis, the sectional properties are obtained by using Hyundai Motor Company's in-house program, and several examples of them are shown in Appendix B.

On the other hand, the original section properties calculated from the software are idealized. It was considered as all parts are assembled perfectly each other. But in the real body structure, most of parts are assembled by spot welding so that there is a difference between the idealized properties calculated by the software and those of the real structure. Therefore, an adjustment is needed. In this thesis, they are reduced to 10 percent for moments of inertia and 30 percent for torsional constant, from original section properties on the basis of I-DEAS User's Manual and the experimental work that have been done by Hyundai Motor Company to correct that problem.

2.2.3 Beam Elements

As it was described previously, beam elements are one-dimensional elements. By using beam elements, the complex structure can be expressed as a simplified skeleton model. But much input data are required to generate beam elements. Like other commercial packages, I-DEAS requires a material property table, a physical property table and a cross-sectional property table. Young's modulus, Poisson's ratio,

and shear modulus can be defined in the material property table, and also beam orientation and offset, and beam end release are defined in the physical property table. Finally, the cross-sectional area, moments of inertia, torsional constant and eccentricity of beam element etc. are defined in the cross-sectional property table.

2.3 Modeling of Panel Parts

The stiffness of the body structure is dominated by members, and in particular, the panel parts are not the main contributors to the bending stiffness. But in the case of torsional rigidity, they affect greatly the in-plane stretching. Generally, frequencies, ω_n, produced by free vibration analysis can be expressed as $\omega_n = \sqrt{k/m}$, where k denotes the stiffness of the body structure and m denotes its mass[4]. This means that frequencies are dominated by stiffness of the body structure and its weight. But panel parts contribute to the weight more greatly than its stiffness, so it is also very important to consider the mass distributions in representing panel parts from the aspect of free vibration analysis.

Panel parts of the body structure are mainly classified by two groups. One of them is almost flat and has simple geometry such as a center floor panel, roof panel, and rear floor panel, etc., and the other one has the complex configurations such as a fender apron panel, shock absorber panel, wheel house panel, cowl parts, etc.. The former ones are represented by rod elements that permit longitudinal degrees of freedom on each node, to consider only the in-plane stretching effect, with neglecting their curvatures. Another way to be able to represent flat panel parts is by using highly

stiffened beam elements, and, in this case, end releases should be imposed on each node to release the three rotational degrees of freedom[5].

On the other hand, to express the latter one, beam elements are used and their beam properties can be obtained by using the following formula

$$D = \frac{E \times t^3}{12(1-\upsilon^2)} \quad \text{----------(2-1)}$$

where t is thickness of parts , E denotes Young's modulus and υ denotes Poisson's ratio. The properties of a plate depend greatly on its thickness, as compared with other dimensions. The quantity D, taking the place of the quantity EI in the case of beams, is called the flexural rigidity of the plate[6].

2.4 Considering of the Joint Flexibility

If the model of the body structure is built by just using beam elements in the skeleton model, it may be often difficult to represent the joint parts, where members are connected by other members. This is because, in the real body structure, these joint parts are designed very smoothly. So, it is possible that these joint parts are modeled too stiff if they are represented by just beam elements. Therefore, flexible joints are applied to compensate for these problems by using rotational spring elements. It is true that the properties of rotational spring elements for the joint parts are obtained by implementation of their detailed model analysis, but it needs much time and efforts to do so. Therefore, in this thesis, those properties are carried over from Hyundai Motor Company's joint stiffness data base.

There are many locations where flexible joints have to be applied in the skeleton model, but for the reason described before, and since the skeleton model has to be constructed in the early design stage, flexible joints are applied on just five locations. They were selected as the front pillar upper to roof side rail, front pillar center to cowl, front pillar lower to side sill , center pillar upper to roof side rail and center pillar lower to side sill, as shown in figure 2.1. In addition, couplings are declared on the nodes where the rotational spring elements are generated to constrain their nodal displacements.

2.5 Units

SI units will be used in this thesis. However, the unit of force will also be expressed and placed in parentheses, in Kilogram-force, or Kgf, for the reason that this unit is used in the test data received from Hyundai Motor Company. The conversion to the SI units is achieved by the relation

$$1 \text{ Kgf} = 9.807 \text{ Newtons} \quad \text{---------- (2-2)}$$

2.6 Weight Adjustments between Real Structure and Skeleton Model

In constructing the skeleton model, there are miscellaneous parts that need not be considered, such as small brackets and flanges for spot welding, which are thought as not contributing to the global stiffness of the body structure. These simplifications cause the weight difference between real structure and skeleton model. This weight

difference does not affect the results of static analysis. But in the free vibration analysis, because of the mass matrix, it may affect the natural frequencies seriously.

Therefore, a weight adjustment is achieved by controlling the mass density of the material properties. For example, the weight for real body structure is 2250.7 N (229.5 Kgf), but the original weight calculated from skeleton model is 1972.9 N (201.2 Kgf). So, 277.5.8 N (28.3 Kgf) of weight difference occurs due to the approximations. By modifying the mass density from 7.82 E3 Kg/m^3 (7.97 E10 $Kgf \cdot sec^2 / mm^4$) to 8.92 E3 Kg/m^3 (9.09 E10 $Kgf \cdot sec^2 / mm^4$), the weight of the skeleton model can be adjusted exactly in the same way as that of the real body structure.

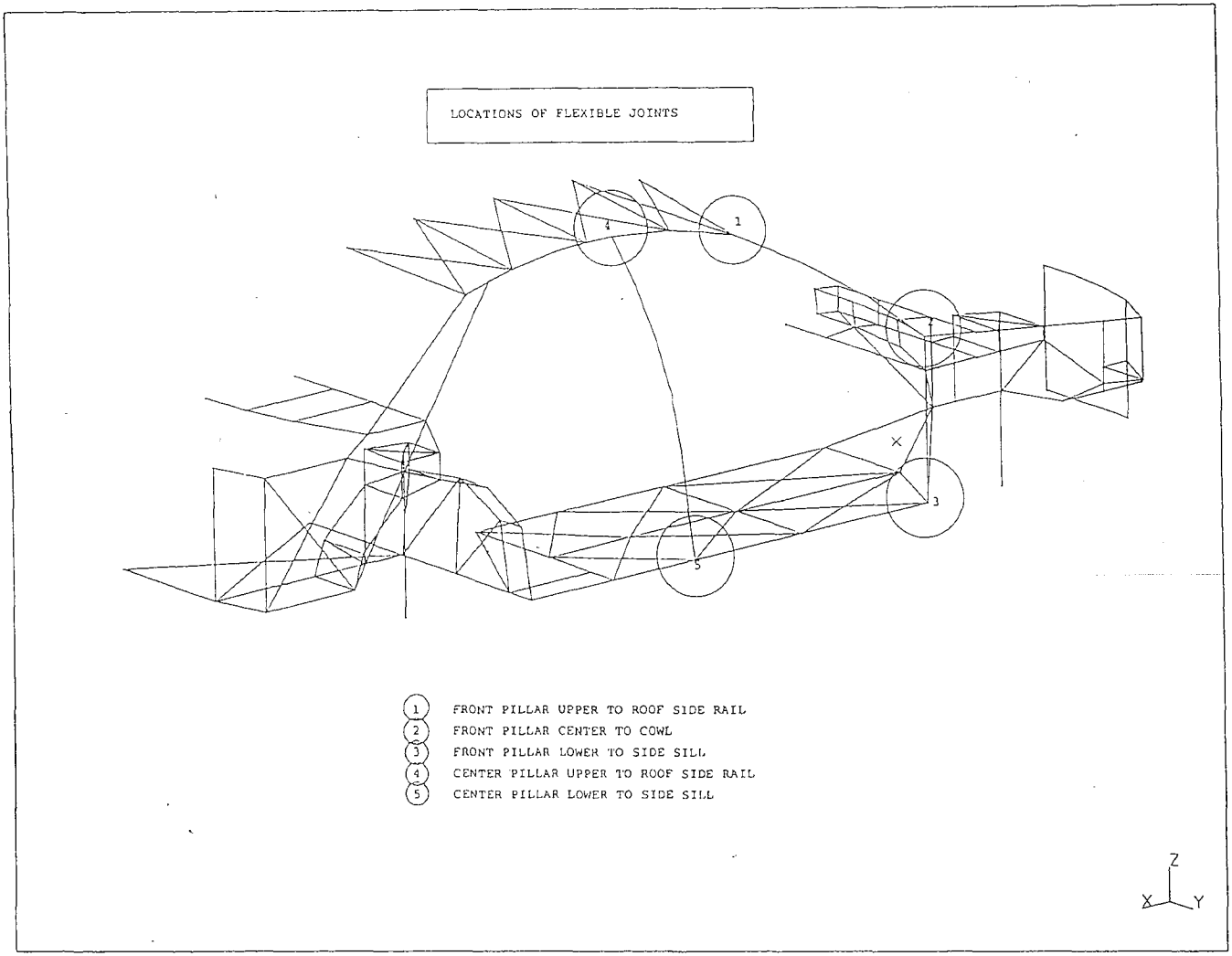

Figure 2.1 Locations of Flexible Joints

Chapter 3

STATIC ANALYSIS FOR THE SKELETON MODEL

3.1 Introduction

To evaluate the stiffness of the body structure for passenger cars, the static bending and torsion tests are implemented according to Hyundai Motor Company's test specifications and procedures. In both tests, the displacements are commonly measured for the applied load cases by using dial gauges, and, from those measured deflections, the static bending stiffness and static torsional rigidity of the body structure for passenger cars are calculated.

In this thesis, the boundary conditions and load conditions are applied in the skeleton model exactly in the same way as the conditions specified in the Hyundai Motor Company's test specifications. Then the displacements needed to calculate the performance of the body structure are obtained.

3.2 Theoretical Basis for Static Analysis

The theory of substructuring is a logical extension of the Gauss elimination method for the solution of linear simultaneous equations and can be found in most standard texts on finite element methods[7-8]. Begin with the simplest form of the static equations of equilibrium :

$$[K]\{U\} = \{F\} \quad \text{----------} \quad (3\text{-}1)$$

where

$[K]$ is the stiffness matrix

$\{U\}$ is the displacement vector

and

$\{F\}$ is the applied force vector

Throughout this thesis, brackets [ ] denote square matrices and { } denote column vectors. The equations may be partitioned into two groups, the master or retained degrees of freedom, here denoted by the subscript "m", and the slave or removed degrees of freedom, here denoted by the subscript "s", as follows:

$$\begin{bmatrix} K_{ss} & K_{sm} \\ K_{ms} & K_{mm} \end{bmatrix} \begin{Bmatrix} U_s \\ U_m \end{Bmatrix} = \begin{Bmatrix} F_s \\ F_m \end{Bmatrix} \quad \text{----------(3-2)}$$

or expanding,

$$[K_{ss}]\{U_s\}+[K_{sm}]\{U_m\}=\{F\} \quad \text{----------(3-3)}$$

$$[K_{ms}]\{Us\}+[K_{mm}]\{U_m\}=\{F_m\} \quad \text{----------(3-4)}$$

Solving equation (3-3) for $\{U_s\}$,

$$\{U_s\}=[K_{ss}]^{-1}\{F_s\}-[K_{ss}]^{-1}[K_{sm}]\{U_m\} \quad \text{----------(3-5)}$$

and substituting for $\{U_s\}$ into equation (3-4) :

$$[[K_{mm}]-[K_s][K_{ss}]^{-1}[K_{sm}]]\{U_m\}$$

$$= [\{F_m\}-[K_{ms}][K_{ss}]^{-1}\{F_s\}] \quad \text{----------(3-6)}$$

or

$$[\overline{K_{mm}}]\{U_m\}=\{\overline{F_m}\} \quad \text{----------(3-7)}$$

where

$$\left[\overline{K_{mm}}\right] = \left[K_{mm}\right] - \left[K_{ms}\right]\left[K_{ss}\right]^{-1}\left[K_{sm}\right] \quad \text{----------(3-8)}$$

$$\left\{\overline{F_m}\right\} = \left\{F_m\right\} - \left[K_{ms}\right]\left[K_{ss}\right]^{-1}\left\{F_s\right\} \quad \text{----------(3-9)}$$

and $\left[\overline{K_{mm}}\right]$, $\left\{\overline{F_m}\right\}$ are the substructure stiffness matrix and load vector, respectively, and may be used in combination with other elements or substructures in an analysis[9]. The resulting displacements $\left\{U_m\right\}$ may then be substituted into equation (3-5) to obtain the displacements $\left[U_s\right]$ in the rest of the substructures.

3.3 Static Bending Analysis

3.3.1 Boundary Conditions

The body structure for passenger cars is symmetric. Therefore, this skeleton model was constructed as a one-half model[10]. In this way, computer time was saved due to the reduced model size and advantages achieved in many other aspects. In the case of static bending analysis, symmetric boundary conditions are applied on the nodes that lie on the center line, namely, the translations x and z, and the rotation y are free, while the translation y and the rotations x and z are fixed. Besides of that, the translation x is free and the rest of five degrees of freedom are fixed as boundary conditions on the front jig point are enforced to match exactly same conditions used in the tests. Also, boundary conditions are declared that rotation y is free and the remaining five degrees of freedom are fixed at the rear jig point. Details are shown in the figure 3.1.

3.3.2 Load Conditions

The static stiffness evaluation was performed to predict the deflection characteristics of the body structure. According to the Hyundai Motor Company's test specifications, there are many types of load conditions. But for the purpose of evaluating the bending stiffness of the body structure for the passenger cars, two load cases are commonly employed in the test to ensure overall bending performance[11].

First one of them is H-point beam load which apply 1962 N (200 Kgf) of force at the hip points of passengers of the front seats. Another one is 4904 N (500 Kgf) of vertical downward load which is applied at the center of wheel base along the side sill. But the load conditions used in this thesis was a modified version of a series of static bending test condition, which has been used successfully to evaluate the performance of the body structure. Instantly, 4904 N (500 Kgf) of vertical load is applied at the side sill and shown in the figure 3.2.

3.3.3 Analytic Results

The results of static bending analysis are shown in figure 3.3. The deformed configuration is shown in figure 3.3, with the peak deflection of 0.774 mm at the side sill under 4904 N (500 Kgf) of the vertical load. The scale used to plot the deformed shape in the figure 3.3 tends to overemphasize the actual deformations.

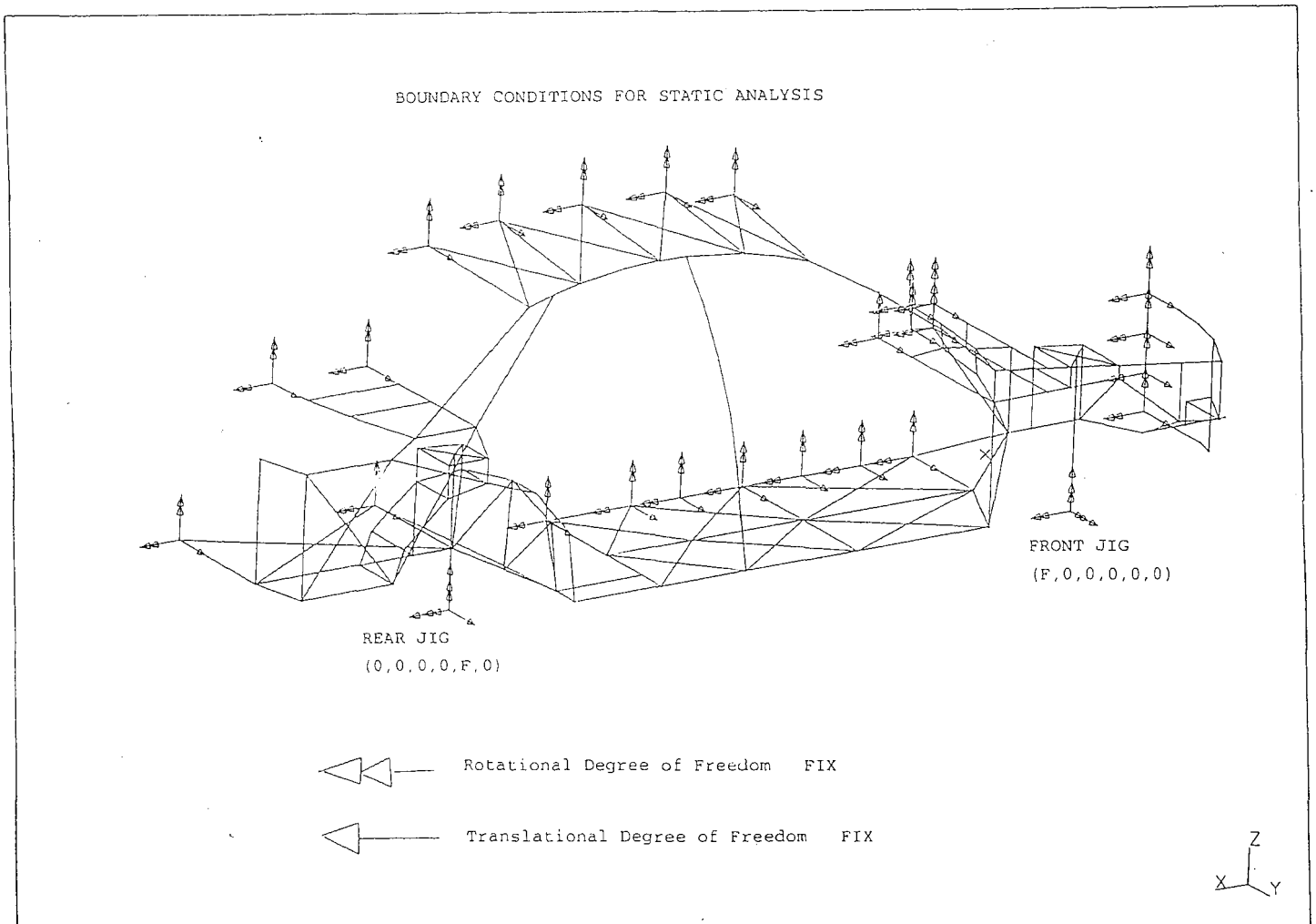

Figure 3.1 Boundary Conditions for Static Bending Analysis

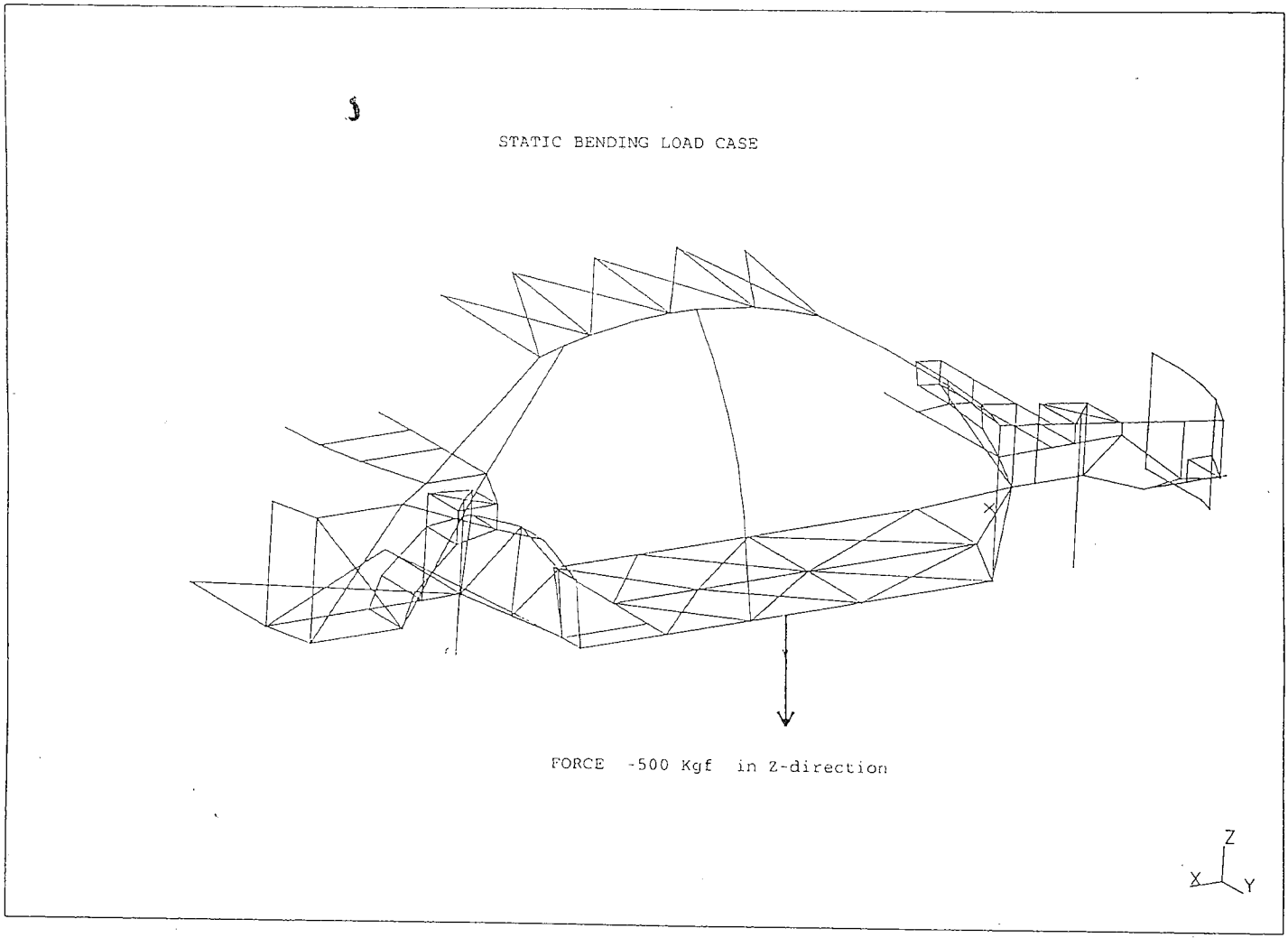

Figure 3.2 Load Condition for Static Bending Analysis

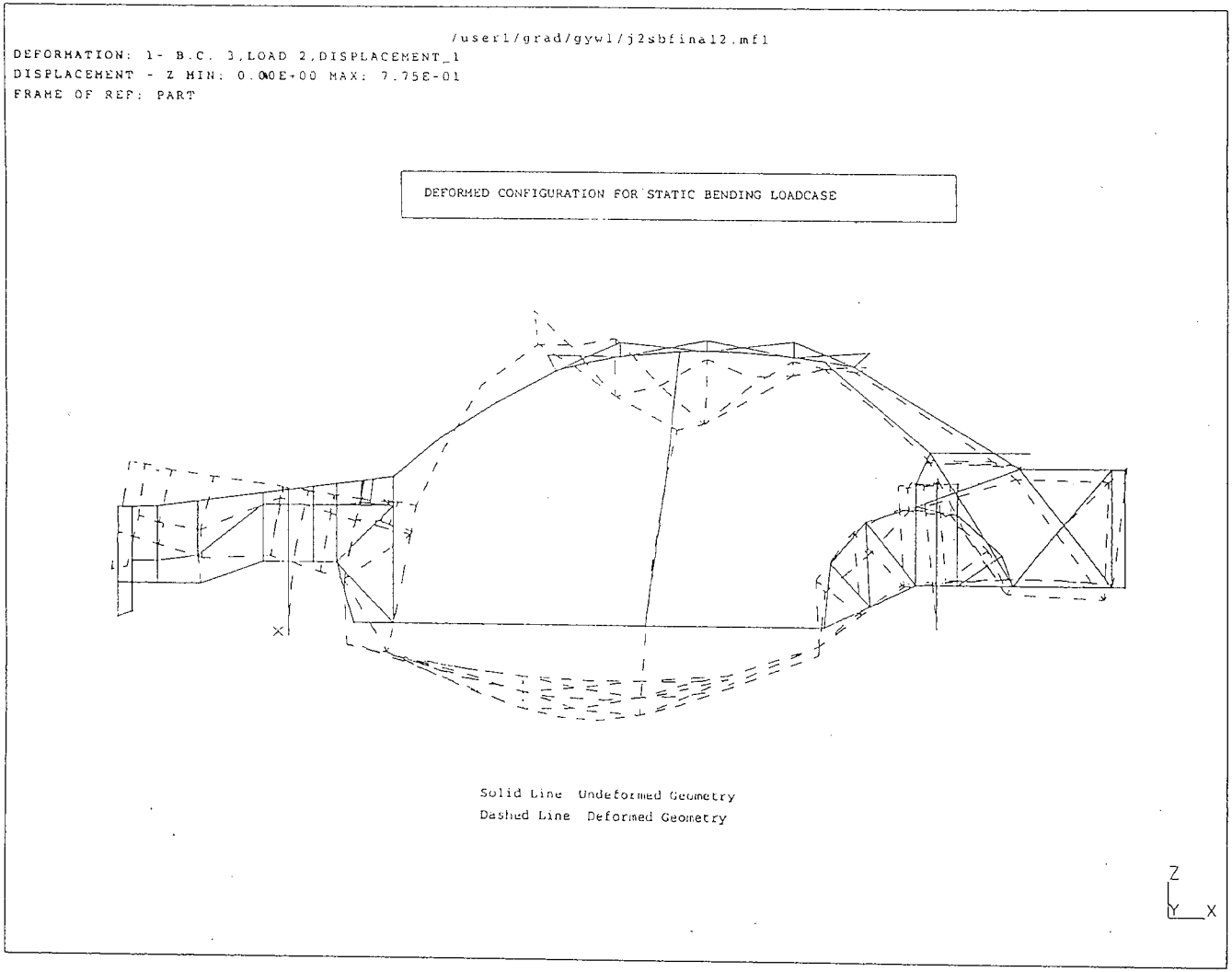

Figure 3.3 Deformed Configuration for Static Bending Loadcase

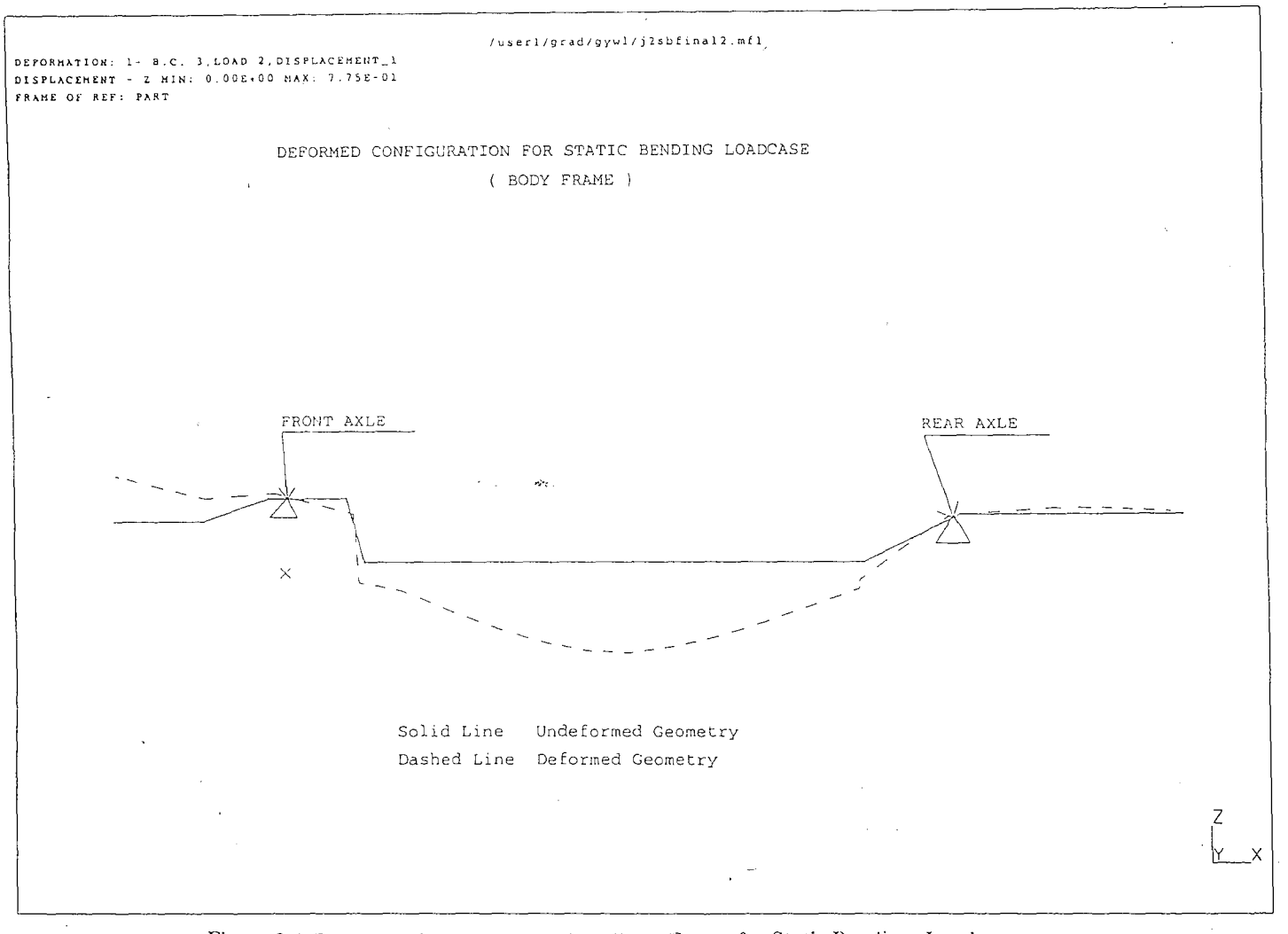

Figure 3.4 Deformed Configuration of the Body Frame for Static Bending Loadcase

However, it does indicate areas which are candidates for change if increased static bending stiffness is required.

On the other hand, if the body structure can be assumed as simply supported beam, then there are no deflections at the front and rear supported locations. But in the case of real test and analysis, small deflections occur at the front and rear axles due to the deformations of jigs for test. Therefore, the original maximum deflection needs to be corrected. After the correction of deformations at the axles, the new maximum deflection is 0.765 mm. From this maximum deflection, the static bending stiffness for the body structure can be calculated from the following formulation[12].

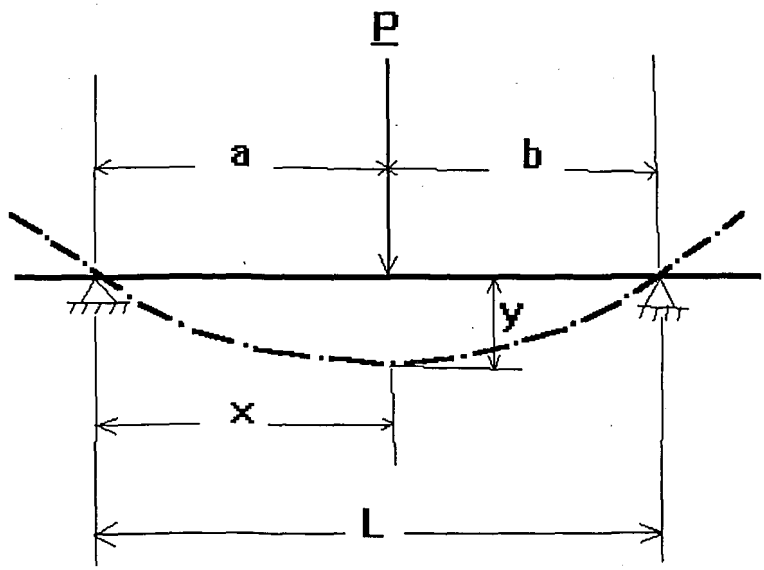

Figure 3.5 Deformed Configuration of the Simply Supported Beam

From above figure 3.5, bending stiffness of the beam, EI, can be expressed as

$$EI = \frac{P \times x \times a(L^2 - x^2 - b^2)}{6 \times L \times y} \quad \text{----------(3-10)}$$

where

P : Applied load

a : Distance between front axle and the location of the applied load

b : Distance between rear axle and the location of the applied load

L : Wheel Base

x : Location of maximum deflection

y : Maximum vertical deflection

Substituting the dimensions and measured deflection into equation (3-10), then static bending stiffness of body structure, EI, is calculated as

$$EI = \frac{4904 \times 1250 \times 1250(2550^2 - 1305^2 - 1245^2)}{6 \times 2550 \times 0.765}$$

$$= 21.85\ \text{E11}\ \text{N} \cdot \text{mm}^2 = 22.28\ \text{E10}\ \text{Kgf} \cdot \text{mm}^2$$

$$= 21.85\ \text{E5}\ \text{N} \cdot \text{m}^2 = 22.28\ \text{E4}\ \text{Kgf} \cdot \text{m}^2$$

3.4 Static Torsion Analysis

3.4.1 Boundary Conditions

As described in static bending analysis, the skeleton model is a one-half model, so antisymmetric boundary conditions are applied at the nodes which lie on center line to perform static torsional analysis. Namely, translation y and rotations x and z are

free, while translations x, z and rotation y are fixed at the nodes of the symmetric plane. Also, according to the test procedure, boundary conditions are declared that rotation x is free and the rest of the five degrees of freedom are fixed at the front jig, while translation x and rotation y are free and the rest four degrees of freedom are fixed at the rear jig. The boundary conditions for static torsional analysis are shown in figure 3.7.

3.4.2 Load Conditions

Torsional behavior of the body structure for the passenger cars is of great significance mainly because of excitations arising out of sources such as rough road conditions, impact loading etc., which often tend to produce a twist in the chassis[13]. The amount of the body structure twist is governed by its ability to resist the twisting moment. This resistance is termed as torsional stiffness and is expressed as torque required to produce a unit twist. According to the test procedure of Hyundai Motor Company for evaluating the static torsional stiffness, 1962 N · m (200 Kgf · m) of torque is applied at the front jig. Detailed configuration for static torsional load case is shown in figure 3.8.

3.4.3 Analytic Results

The results of static torsional analysis are shown in figure 3.9 through 3.11. The deflected configuration is shown in figure 3.9 with the vertical deflection of 2.27

mm at the front axle. According to following three steps, the torsional rigidity of the body structure, GJ, can be calculated from this deflection at the front axle.

Step 1. Derivation of twisting angle θ

From following figure 3.6, twisting angle, θ , can be defined as

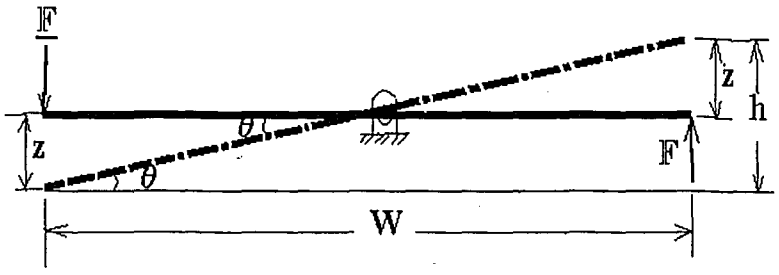

Figure 3.6 Torsional Configuration of Beam

$$\theta = \mathrm{Tan}^{-1}\left(\frac{2z}{W}\right) \text{ ----------(3-11)}$$

where

z : Vertical deflection at the front axle

W : Wheel tread of a car

Substituting the measured deflection and dimension of the wheel tread into equation (3-11), then the angle of twist is obtained as

$$\theta = \frac{4.54}{949} \times \frac{180}{\pi} \times 60$$

$$= 16.4^{\circ}$$

Step 2. Calculation of torsional stiffness

Torsional stiffness of body structure can be defined as

$$K = \frac{T}{\theta} \times 60 \text{ ----------(3-12)}$$

where

K : Torsional stiffness

T : Applied torque

θ : Angle of twist

Substituting applied torque and twisting angle calculated from equation (3-11), then torsional stiffness, K, becomes

$$K = \frac{1962}{16.4} \times 60$$

$$= 7172.8\ \mathrm{N \cdot m / deg} = 731.4\ \mathrm{Kgf \cdot m / deg}$$

Step 3. Calculation of torsional rigidity

Torsional rigidity of the body structure, GJ, can be defined as

$$GJ = K \times L \times \frac{180}{\pi} \quad \text{----------(3-13)}$$

where

L : Wheel base of a car

Substituting the value of torsional stiffness and dimension of wheel base into equation (3-13), then finally torsional rigidity of the body structure for the passenger cars becomes

$$GJ = 7172.8 \times 2.55 \times \frac{180}{\pi}$$

$$= 1049201.8\ \mathrm{N \cdot m^2 / rad} = 106985.7\ \mathrm{Kgf \cdot m^2 / rad}$$

Therefore, for a given body structure with appropriate support conditions, if value of z are measured for a corresponding set of F values of applied loads, the torsional rigidity as given above can be calculated.

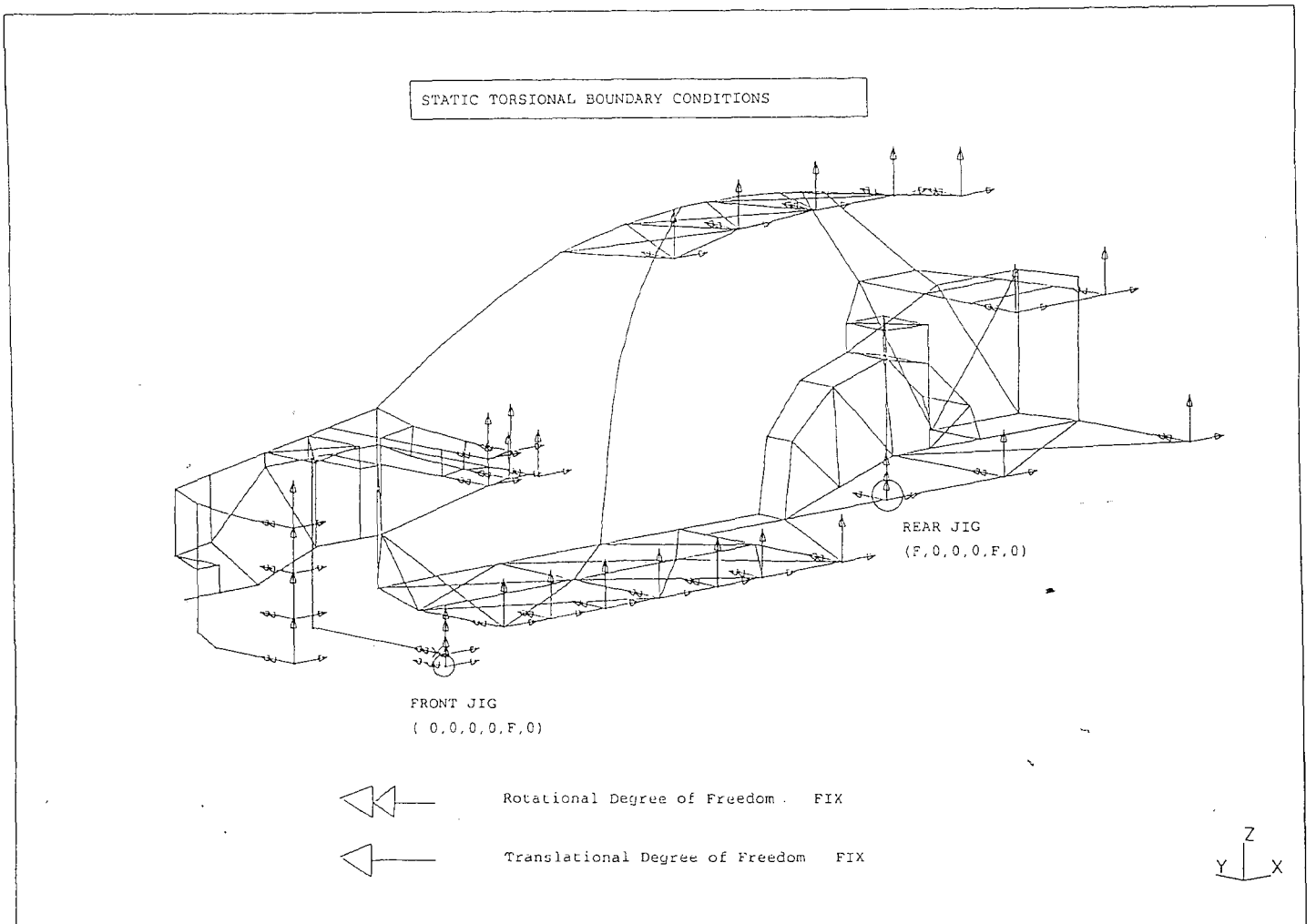

Figure 3.7 Boundary Conditions for Static Torsional Analysis

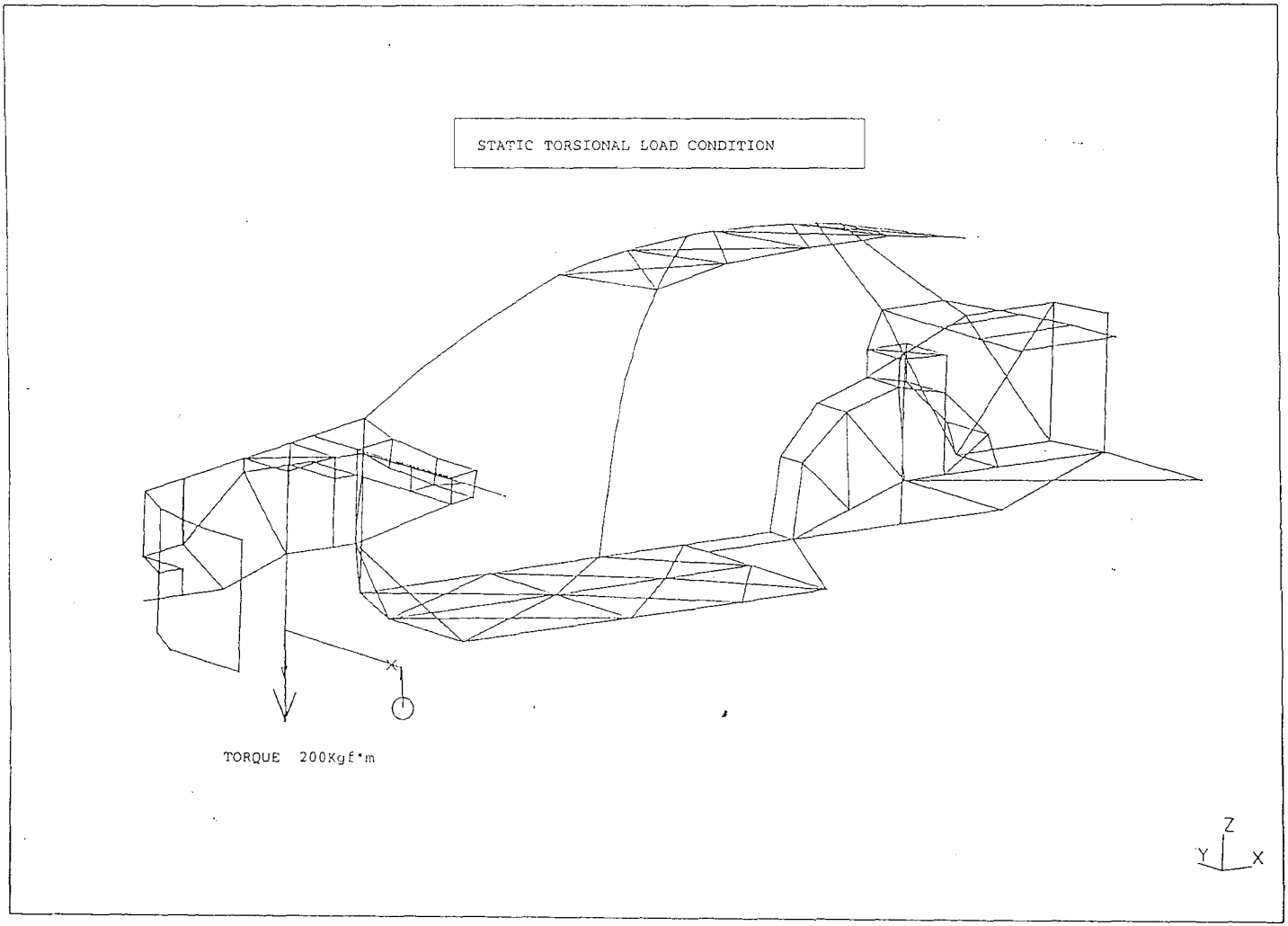

Figure 3.8 Load Condition for Static Torsional Analysis

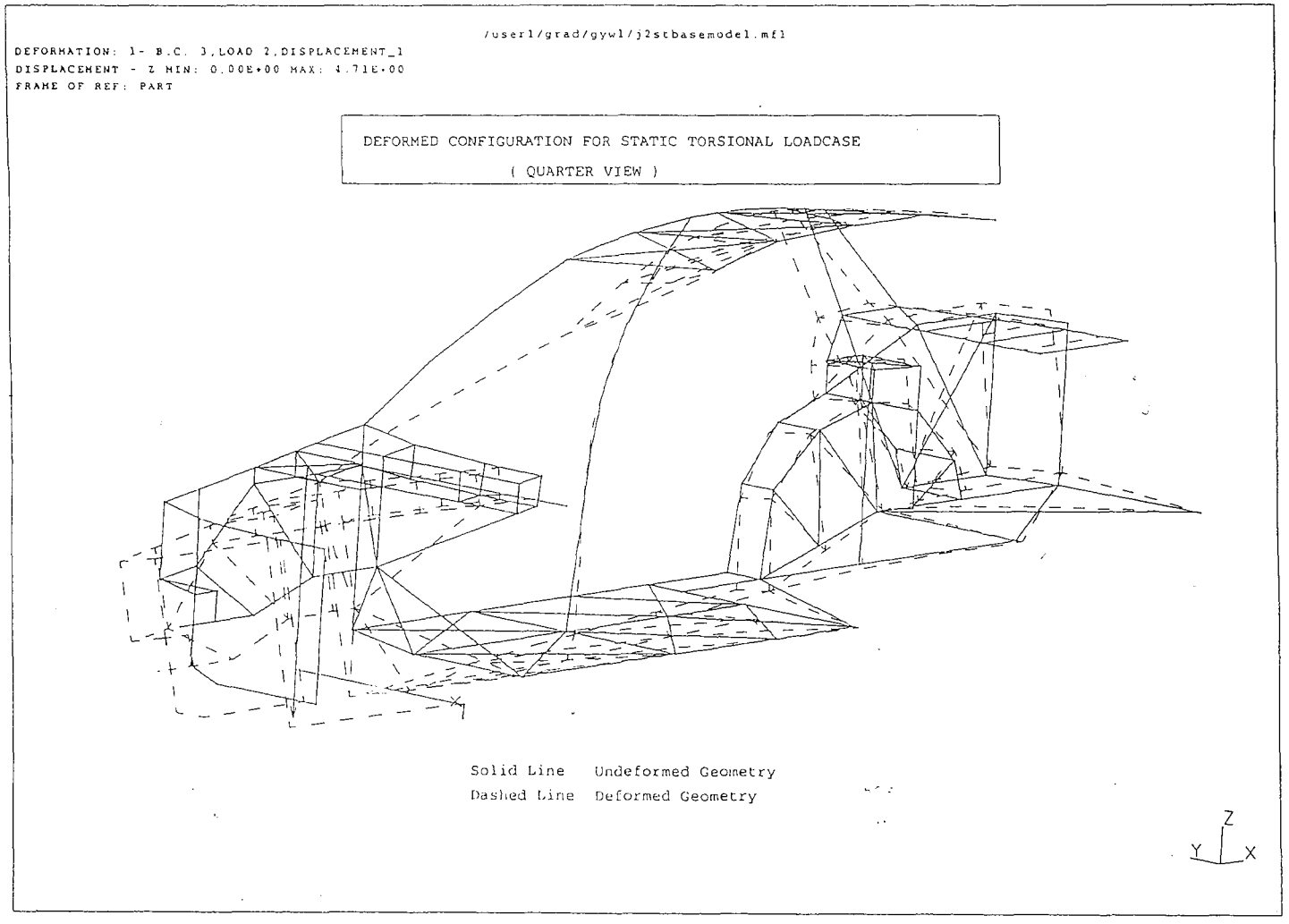

Figure 3.9 Deformed Configuration for Static Torsion Loadcase (Quarter View)

/user1/grad/gywl/j2stbasemodel.mf1

DEFORMATION: 1- B.C. 1,LOAD 2,DISPLACEMENT_1
DISPLACEMENT - Z MIN: 0.00E+00 MAX: 4.71E+00
FRAME OF REF: PART

DEFORMED CONFIGURATION FOR STATIC TORSIONAL LOADCASE
(FRONT VIEW)

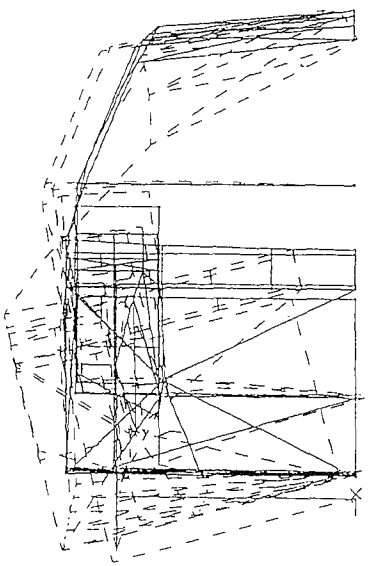

Solid Line Undeformed Geometry
Dashed Line Deformed Geometry

Figure 3.10 Deformed Configuration for Static Torsion Loadcase (Front View)

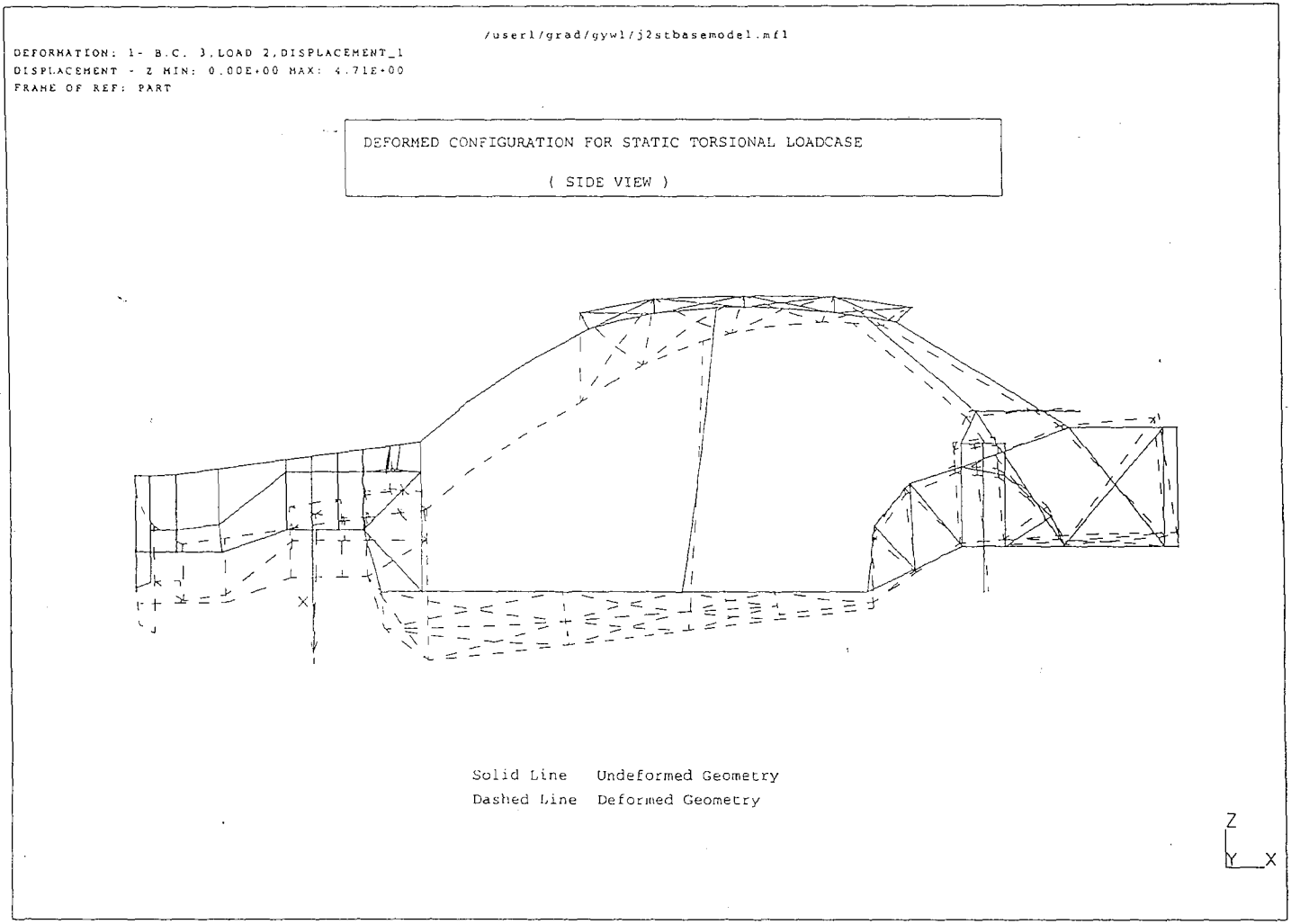

Figure 3.11 Deformed Configuration for Static Torsion Loadcase (Side View)

Chapter 4

FREE VIBRATION ANALYSIS FOR SKELETON MODEL

4.1 Introduction

The objective of the free vibration analysis is to obtain analytically the bending and torsional frequencies and their corresponding modes for the body structure of a passenger car. The modal vibration behavior of an automobile has been shown to be significant in its influence on the idle, shake, and shimmy vibration of full vehicles. During design, knowledge of the natural modes of vibration is valuable to the engineers, and the analytically predicted modes can be synthesized with experimental data to provide guidelines for automobile vibration[14]. To predict the natural frequencies of the body structure in the early design stage is very important, because it is possible to avoid the resonance between natural frequencies of the body structure and those of the engine as well as the exhaust system, which are the main sources of automobile vibration.

4.2 Theoretical Basis for Free Vibration Analysis

The general form of the equations of motion for dynamics is

$$[M]\{\ddot{U}\} + [C]\{\dot{U}\} + [K]\{U\} = \{F\} \quad \text{----------(4-1)}$$

where

$[M]$: Mass matrix

$[C]$: Damping matrix

$[K]$: Stiffness matrix

$\{\ddot{U}\}$: Acceleration vector

$\{\dot{U}\}$: Velocity vector

$\{U\}$: Displacement vector

For free vibration analysis, there are no external forces, and if the damping factor of the body structure is neglected, then equation (4-1) is reduced to

$$[M]\{\ddot{U}\} + [K]\{U\} = \{0\} \quad \text{----------(4-2)}$$

If free vibration in the N degrees of freedom is assumed as a simple harmonic motion, then the solution for the N degrees of freedom can be written as

$$\{U\} = \{\phi\} \sin \omega_n \ (t - t_0) \quad \text{----------(4-3)}$$

where

n = 1,2, ,,, N

$\{\phi\}$: N^{th} order vector

ω_n : natural frequencies of their corresponding to the mode shapes

Substituting equation (4-3) into equation (4-2), then a generalized eigenvalue problem[15] is obtained in the form of

$$[K]\{\phi\} = \omega_n^2 [M]\{\phi\} \quad \text{----------(4-4)}$$

or by the Rayleigh quotient for the frequency of vibration

$$\omega_n^2 = \frac{[\phi]^T [K][\phi]}{[\phi]^T [M][\phi]} \quad \text{----------(4-5)}$$

where

$[\phi]^T$: transposed matrix of $[\phi]$

From equation (4-4) and (4-5), N natural frequencies and their corresponding mode shapes are obtained and, for substructuring, an equation of the form is needed.

$$[\overline{M_{mm}}]\{\ddot{U}_m\} + [\overline{K_{mm}}]\{U_m\} = \{0\} \quad \text{----------(4-6)}$$

Simple partitioning and condensation are not practical, primarily because the condensed matrices are functions of the time derivatives of the displacements and very awkward to compute. The condensations used for substructuring in actual practice are therefore approximate, but give generally acceptable results provided the master degrees of freedom have been judiciously chosen. Almost universally, $[\overline{K_{mm}}]$ is computed in the same way as for the static case. There is considerable variation, however, in the computation of the reduced mass matrices[16].

On the other hand, normal modes of free vibration analysis can be derived from several different formulations to obtain undamped natural frequencies and their corresponding modes of vibration and there are three solution methods used in I-DEAS

software to obtain them[17]. First one is the Simultaneous Vector Iteration (SVI) formulation and a single iteration in the simultaneous vector iteration algorithm, consisting of two steps :

- Step 1. Inverse power

$$[\psi] = [K]^{-1}[M][\phi]_{old} \quad \text{----------(4-7)}$$

- Step 2. Subspace orthogonalization

$$[\phi]_{new} = [\psi][Q] \quad \text{----------(4-8)}$$

where

$$[\psi]^T [K][\psi][Q] = [\psi]^T [M][\psi][Q][\lambda] \quad \text{----------(4-9)}$$

and

$[\psi]^T [K][\psi]$: stiffness inner products

$[\psi]^T [M][\psi]$: mass inner products

$[\phi]$ is a matrix whose columns represent the mode shape estimates and whose rows correspond to unrestrained degrees of freedom, and $[Q]$and $[\lambda]$ are eigenvectors and eigen values of the mass and stiffness inner product matrices[18]. As iteration proceeds, the columns of $[\phi]$ and terms in $[\omega]$ converge to the modes and frequencies of the finite element model. Note that no static condensation approximation is performed and, technically, the terms in $[\omega]$ are frequencies squared, in radians.

Next solution method is the Guyan reduction formulation. It was described previously about the static condensation approximation in the theoretical basis for static analysis of the chapter 3, and it is the heart of the Guyan reduction method[19].

Let

$$\begin{bmatrix} M_{mm} & M_{ms} \\ M_{sm} & M_{ss} \end{bmatrix} \begin{Bmatrix} \ddot{U}_m \\ \ddot{U}_s \end{Bmatrix} + \begin{bmatrix} K_{mm} & K_{ms} \\ K_{sm} & K_{ss} \end{bmatrix} \begin{Bmatrix} U_m \\ U_s \end{Bmatrix} = \begin{Bmatrix} 0 \\ 0 \end{Bmatrix} \quad \text{----------(4-10)}$$

where also 's' subscripts denote slave partitions and 'm' subscripts denote master partitions. The inertia forces of the slave partitions are small compared to the elastic forces of the master. The static condensation approximation is

$$M'_{ms} \approx 0, \qquad M_{ss} \approx 0 \quad \text{----------(4-11)}$$

The bottom set of the equations is solved to yield

$$U_s = [G]U_m \quad \text{----------(4-12)}$$

where

$$[G] = -[K_{ss}]^{-1}[K_{sm}] \quad \text{----------(4-13)}$$

which can be written as

$$\begin{bmatrix} U_m \\ U_s \end{bmatrix} = \begin{bmatrix} [I] \\ [G] \end{bmatrix} U_m \quad \text{----------(4-14)}$$

where

$[I]$: Identity matrix

Assume for the moment that the mass matrix is diagonal or nearly so. Then equation (4-11) suggests that master degrees of freedom should be chosen at nodes where mass

is relatively large. This situation occurs, for example, where lumped mass elements have been added to a structure. Equation (4-13) requires that the slave partition be invertible, and it means that the master degrees of freedom must be chosen such that, if they were to be treated as restraints, then no rigid body motion would be possible. Assume next that the stiffness matrix is diagonal, or at least diagonally dominant, and has large diagonal terms. This situation implies that the numbers in $[G]$ are smaller than the numbers in $[I]$. Now examine the matrix in equation (4-14). All Guyan modes will be linear combinations of the columns in this matrix. The largest terms in these columns occur at the master degree-of- freedom locations, which suggests that it is desirable to have master degrees of freedom at nodes where the exact mode shape deflections are large. Previous solutions, structural symmetry, and past experience are sources for estimating where these locations might be. The remainder of the Guyan reduction algorithm consists of using equation (4-14) to construct a reduced set of mass and stiffness matrices. The number of rows and columns in these matrices is equal to the number of master degrees of freedom. A schematic representation follows

$$\left[[I][G]^T\right]\begin{bmatrix} M_{mm} & M_{ms} \\ M_{sm} & M_{ss} \end{bmatrix}\begin{bmatrix} [I] \\ [G] \end{bmatrix}\ddot{U}_m$$

$$+\ \left[[I][G]^T\right]\begin{bmatrix} K_{mm} & K_{ms} \\ K_{sm} & K_{ss} \end{bmatrix}\begin{bmatrix} [I] \\ [G] \end{bmatrix} U_m = \begin{Bmatrix} 0 \\ 0 \end{Bmatrix} \text{ ----------(4-15)}$$

where

$$\left[[I][G]^T\right]\begin{bmatrix} M_{mm} & M_{ms} \\ M_{sm} & M_{ss} \end{bmatrix}\begin{bmatrix} [I] \\ [G] \end{bmatrix} : \text{reduced mass matrix,}$$

$$\left[[I][G]^T\right]\begin{bmatrix} K_{mm} & K_{ms} \\ K_{sm} & K_{ss} \end{bmatrix}\begin{bmatrix} [I] \\ [G] \end{bmatrix} : \text{reduced stiffness matrix}$$

An eigenvalue extraction algorithm is used to obtain the modes and frequencies of the reduced problem[20]. The full mode shapes are obtained using equation (4-12). The Householder QL extraction is performed in memory, which places a limit on the number of master degrees of freedom, which can be selected. This limit is specific to each computer system. A check to see if enough space is available is made after *Solve* is picked, but before the analysis begins. This limit is large enough, so that, when it is encountered, an Simultaneous Vector Iteration solution is more efficient.

The final solution method is the Lanczos formulation. The purpose of the Lanczos method is to compute a relatively few eigenvalue and eigenvector pairs for a model defined by a large number of degrees of freedom[21]. By using restart solutions coupled with frequency shifting, a large number of modes can be determined efficiently by obtaining a few at a time. The Lanczos method has the property that well-isolated eigenvalues are approximated accurately after a comparatively small number of steps. The eigenvalues most frequently wanted are the smaller ones. And the Lanczos algorithm has the ability to compute the smaller eigenvalues of a matrix without any factorization. However, they will not be approximated accurately until nearly all eigenvalues have been determined. Consequently, it is necessary to apply Lanczos factorization to an inverted form of the matrix. In this respect, the Lanczos method is

just like the subspace iteration method. The Lanczos algorithm uses a shift-and-invert procedure to converge quickly to the eigenvalues closest to the shift, and the eigenvectors of the original and shifted problem are the same. As it was mentioned before, the general eigenproblem is

$$K x = \lambda M x \quad \text{----------(4-16)}$$

Applying a shift, the algorithm works with the equation

$$\overline{K}\ x = \nu M x \quad \text{----------(4-17)}$$

where

$$\overline{K} = K - \sigma M \quad \text{----------(4-18)}$$

Since the algorithm works this the inverse of $\overline{K}$, the spectrum of the original eigen problem is related to the spectrum of the shifted problem by

$$\lambda = \frac{1}{\nu - \sigma} \quad \text{----------(4-19)}$$

The Lanczos method can be thought of as a means of constructing an orthogonal set of vectors, known as Lanczos vectors, for use in the Rayleigh-Ritz procedure. The algorithm is closely related to the inverse iteration and power methods for calculating a single eigenpair. Given a pair of matrices

$$\overline{K} = K - \sigma M \text{ and } M \quad \text{----------(4-20)}$$

and a starting vector r, these basic methods generate a sequence of vectors

$$\left\{r, \left[\overline{K}^{-1} M\right] r, \left[\overline{K}^{-1} M\right] 2r, ,,,,, \left[\overline{K}^{-1} M\right] jr\right\} \quad \text{----------(4-21)}$$

during j iterations. These vectors are referred to as the Krylov sequence and the sequence converges to the eigenvector corresponding to the eigenvalue, λ, closest to the shift σ as j goes to infinity. The basic difference between the Lanczos method and the other two methods is that the information contained in each successive vector of the Krylov sequence is used to obtain the best approximation to the wanted eigenvectors instead of using only the last vector in the sequence[22]. In other words, the Lanczos algorithm is equivalent to obtaining the Rayleigh-Ritz approximation with the vector in the Krylov sequence as the trial vectors. This method involves supplementing the Krylov sequence with an orthogonalization process with respect to the other vectors. The result is a set of M-orthonormal vectors that is used in the Rayleigh-Ritz procedure to reduce the dimension of the eigenvalue problem. The Rayleigh-Ritz procedure, with the M-orthonormal basis of the Krylov subspace, leads to a standard eigenvalue problem with a tri-diagonal matrix.

4.3 Results of Free Vibration Bending Analysis

In the case of free vibration analysis, the concerns are to obtain the fundamental frequencies and their corresponding mode shapes which influence the free vibration of a full vehicle. Characteristics of the first bending mode are the following. First, it has the nodal points close to the suspension lines, which are described as front and rear axles. Second, the maximum curvature occurs at the top of the front pillar[23]. It looks almost like a hinge because flexible joints are applied in this locations. However, it is important to know that the objective of this analysis is to obtain the major bending

modes. Therefore, local modes such as those that take place in the area of roof front and rear rail, center floor, rear floor trunk well etc., are of less interest. From the results of free vibration bending analysis, its first natural bending frequency is 41.5 Hz, and the corresponding mode shape is shown in figure 4.1.

4.4 Results of Free Vibration Torsional Analysis

As described in the previous section, the purpose of free vibration torsion analysis is also to obtain its fundamental frequencies and their corresponding mode shapes which influence on the shimmy vibration in the system of a full vehicle. The characteristics of the first torsion mode are large lateral coupling, especially at the roof, which is moving from side to side and the lateral shape resembles that of the first lateral bending mode. Another feature that has to be inspected carefully is whether nodal points occur at the upper structure, such as the roof and the lower structure, center floor panel, or the rear floor panel, as seen from the side view due to the torsional behavior. From the results of the free vibration analysis, its first torsional frequency is 25.5 Hz, and the corresponding mode shape is shown in figure 4.2 through figure 4.5.

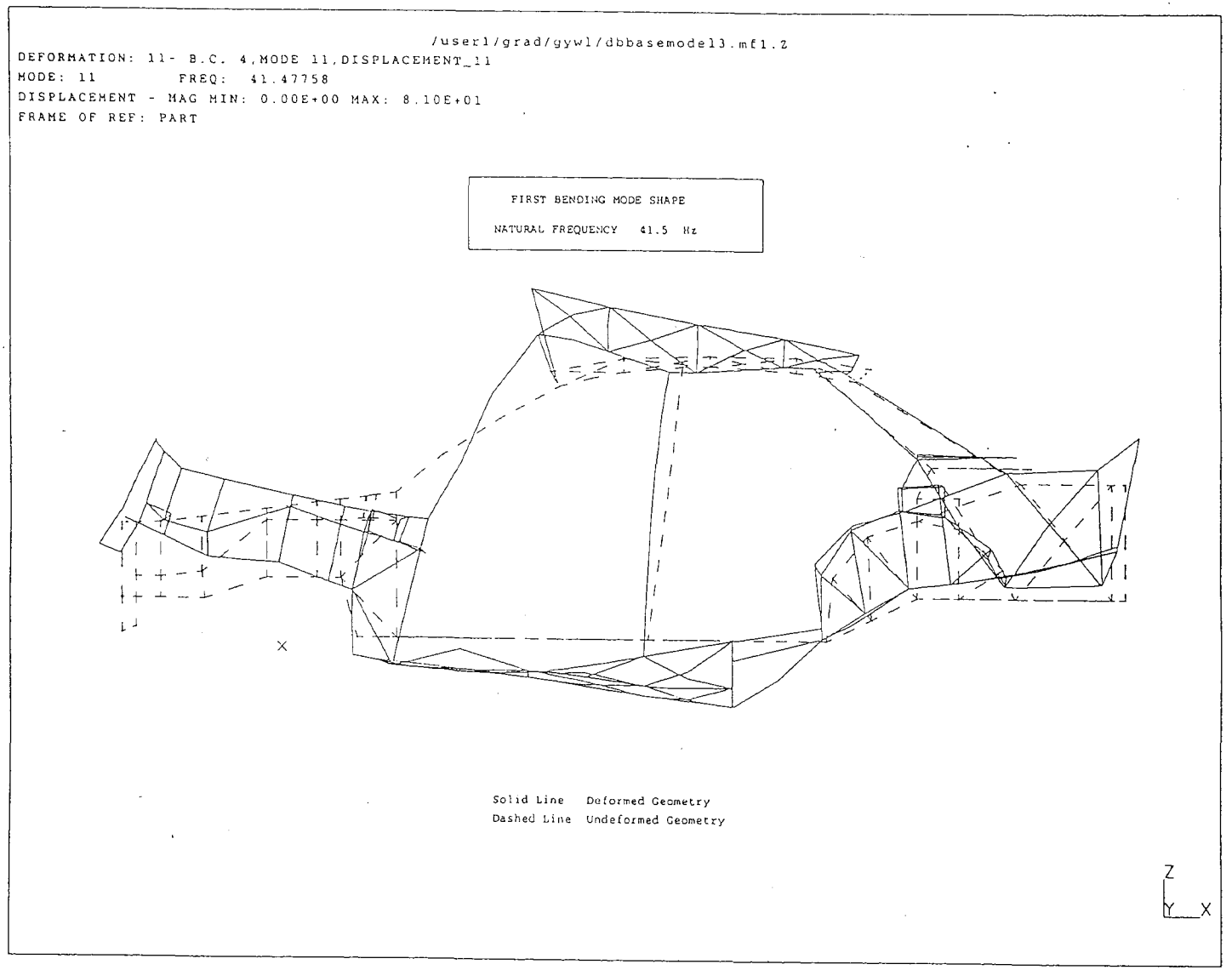

Figure 4.1 Configuration of First Bending Mode Shape

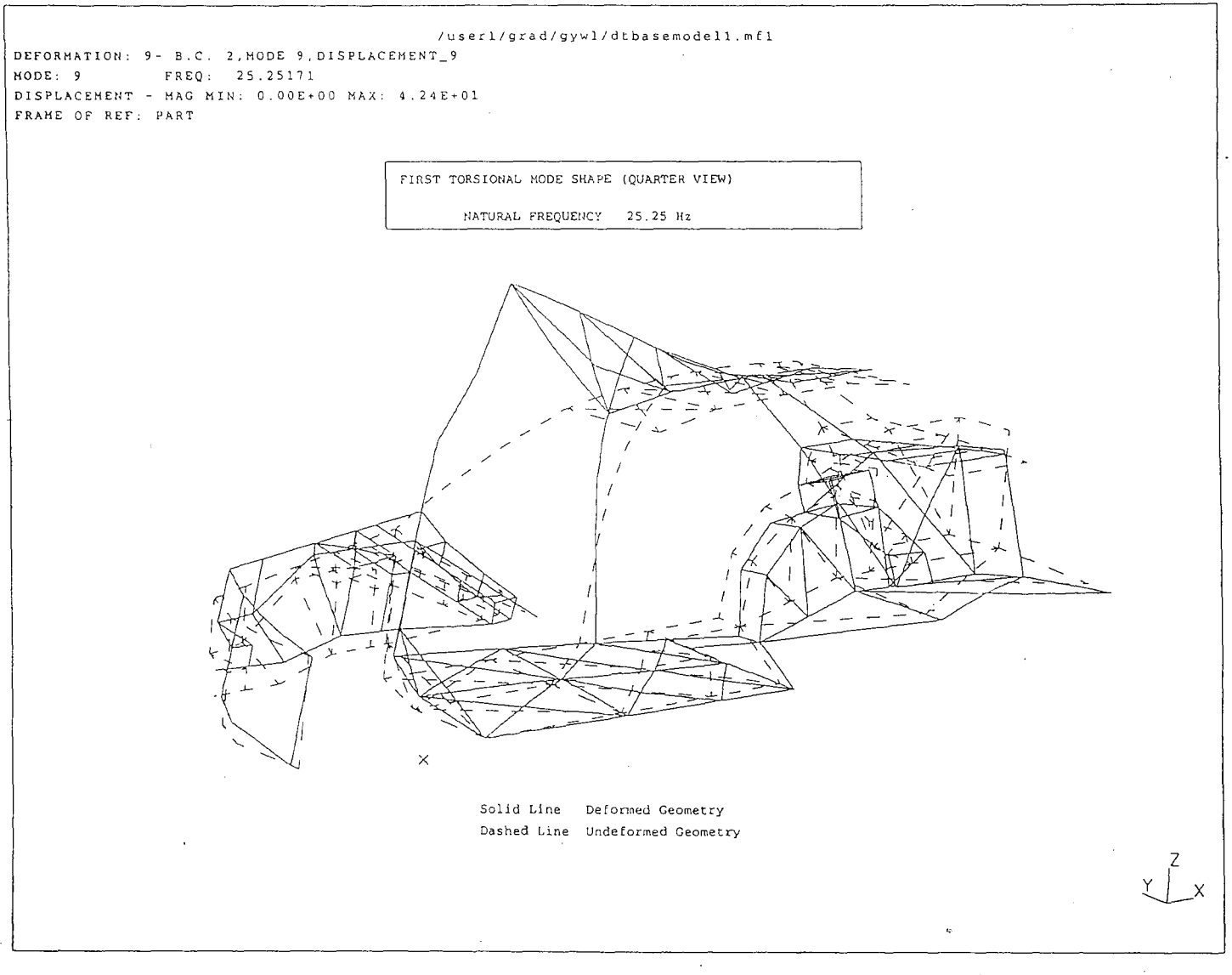

Figure 4.2 Configuration of First Torsional Mode Shape (Quarter View)

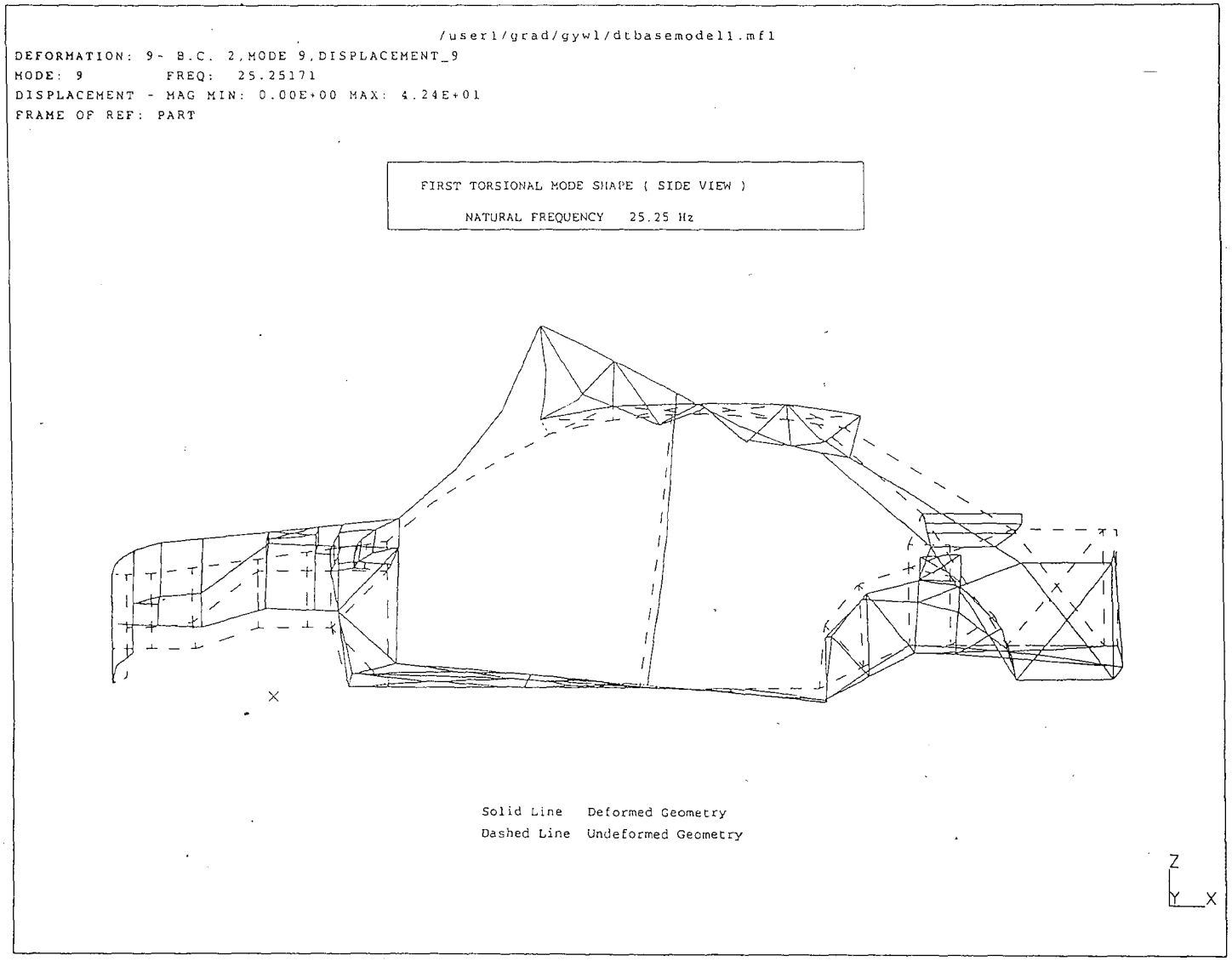

Figure 4.3 Configuration of First Torsional Mode Shape (Side View)

/user1/grad/gywl/dtbasemodel1.mf1
DEFORMATION: 9- B.C. 2,MODE 9,DISPLACEMENT_9
MODE: 9 FREQ: 25.25171
DISPLACEMENT - MAG MIN: 0.00E+00 MAX: 4.24E+01
FRAME OF REF: PART

FIRST TORSIONAL MODE SHAPE (FRONT VIEW)
NATURAL FREQUENCY 25.25 Hz

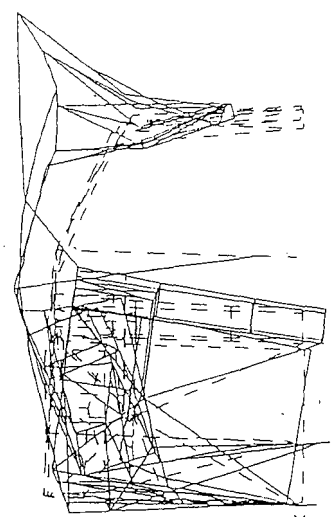

Solid Line Deformed Geometry
Dashed Line Undeformed Geometry

Figure 4.4 Configuration of First torsional Mode Shape (Front View)

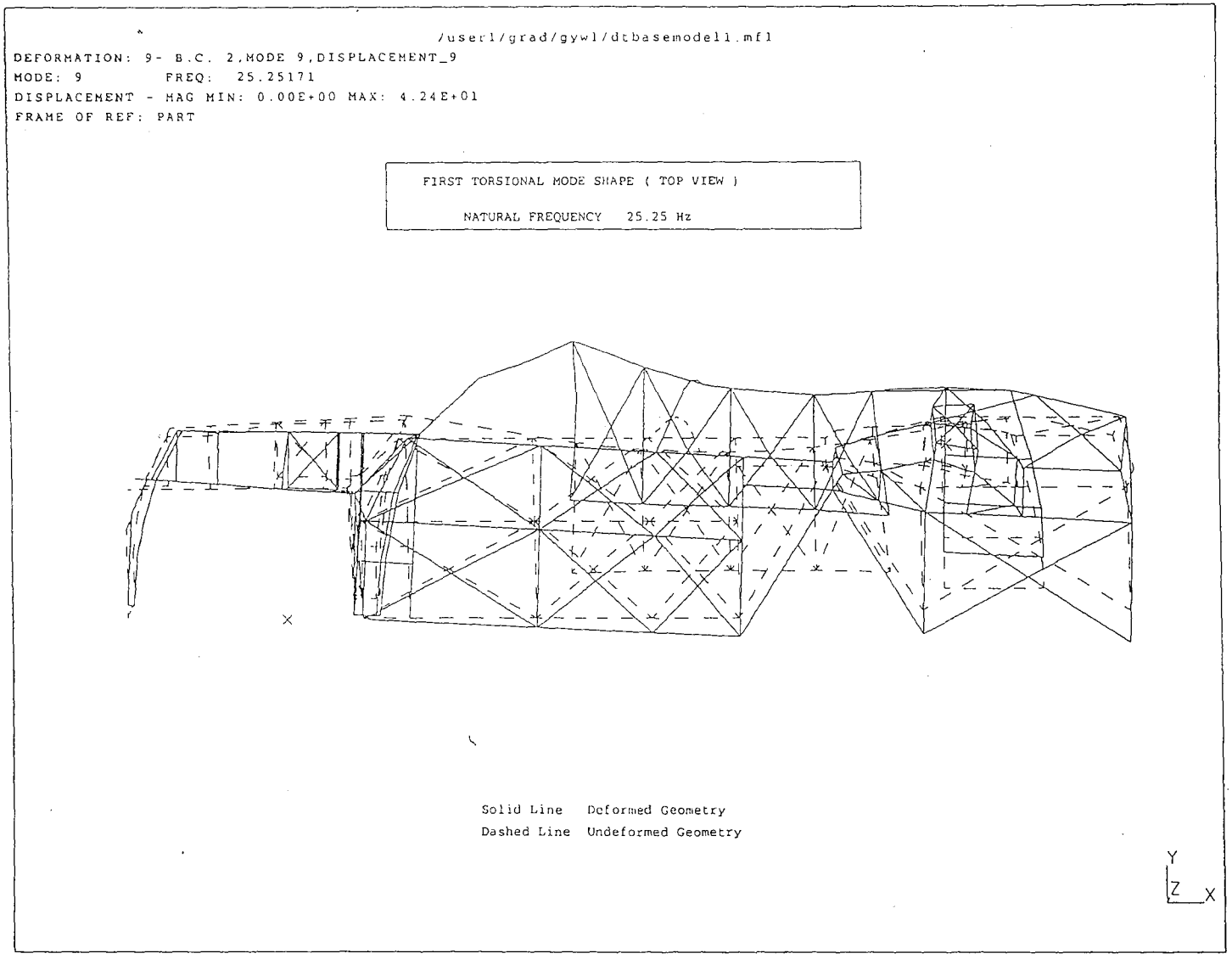

Figure 4.5 Configuration of First torsional Mode Shape (Top View)

Chapter 5

COMPARISON OF RESULTS BETWEEN ANALYSIS AND TEST

5.1 Results for Static Analysis

In order to verify whether the analytic results of this skeleton model are reasonable or not, it is necessary to demonstrate the validity of these analytic results. A full-scale, prototype body structure was fabricated for test and demonstration purposes by Hyundai Motor Company, so that the analytic results can be compared with those of the test. In the case of static bending stiffness, the global behavior of deformation of the main frame of the body structure was compared. As shown in figure 5.1, the trend of deformations for the analytic results is almost the same as that of test results, but the maximum anâlytic deflection at side sill is 0.765 mm, while the maximum deflection obtained by test is 0.708 mm. However, the location at which the maximum deflection is calculated and measured is not exactly the same. The deflection was calculated at the location of x=1035 mm, while it was measured at the location of x=1025 mm. From both maximum deflections, the static bending stiffness for analysis and test are calculated, and their results are 21.85E5 $N \cdot m^2$ (22.84E4 $Kgf \cdot m^2$), 22.12E5 $N \cdot m^2$ (22.56E4 $Kgf \cdot m^2$), respectively.

In the case of static torsional rigidity, the twisting angle distributions of the body frame was also compared between analysis and test. The results are shown in figure 5.2. The analytic twisting angle at the front axle is 16.4 ° , while that obtained by

test is 13.5 . From those results, the torsional rigidities for both analysis and test are derived, and their results are 10.5E5 $N \cdot m^2$/ rad (10.7E4 $Kgf \cdot m^2$/ rad), 12.7E5 $N \cdot m^2$/ rad (12.98E4 $Kgf \cdot m^2$/ rad), respectively.

Also, all results of analysis and test for static load cases are summarized in Table 5.1. From the results in Table 5.1, it can be concluded that, in the case of static analysis, the analytic results are satisfactory, with percent errors of 2 % for the static bending load case and 16 % for the static torsional load case. It can be seen that the results of the static bending case are more accurate than those of the static torsional case.

Load case	Contents	Analysis	Test
Static bending	Maximum deflection	0.765 mm	0.708 mm
	Static bending stiffness	21.85E5 $N \cdot m^2$	22.12E5 $N \cdot m^2$
	Accuracy	98 %	100 %
Static torsion	Twisting angle	16.4	13.5
	Torsional rigidity	10.5E5 $N \cdot m^2$/ rad	12.7E5 $N \cdot m^2$/ rad
	Accuracy	84 %	100 %

Table 5.1 Comparison of results for static load cases

5.2 Results for Free Vibration Analysis

Although the static stiffness characteristics of the body structure were examined experimentally, the primary method used to evaluate the accuracy of the finite element skeleton model is the free vibration test. The vibration data for the body structure are compared with those of the analytical results in the following Table 5.2.

Mode	Frequencies (Hz)		
	Analysis	Test	Accuracy
First bending	41.5	44.4	93 %
First torsion	25.3	28.5	88 %

Table 5.2 Frequency comparison between analysis and test

It is seen from the results in Table 5.2 that the percent errors are 7 % for the first bending frequency and 12 % for the first torsional frequency. Furthermore, the mode

shapes were found to be in satisfactory agreement. The experimental verification of the body structure was considered to be exceptionally good.

5.3 Improvement of analytic results

It can be expected that the flexibility assigned to flexible joints will affect greatly the analytic results in the skeleton model. Therefore, it is very important to decide how to represent the flexible joints. As it was described previously, there are five locations at which flexible joints are applied in the body structure, and they are represented as rotational spring elements. The use of the flexible joints at the critical joints, where more than three beam elements are connected, is reasonable. But in real structure, the connecting parts to the flexible joints are very stiff, when compared to ordinary beam elements that are away from the flexible joints. This implies that treating the connecting beam elements in the same manner as ordinary beam elements may not be suitable for an accurate analysis.

Therefore, in this thesis, those beam elements that surround the flexible joints were modified as rigid beam elements, as shown by the heavy solid lines in figure 5.3. Then the original analytic results for free vibration analysis were improved considerably. These results are summarized in Table 5.3. They show that it is more accurate to represent the surrounding beam elements of the flexible joints as rigid elements.

Mode	Frequencies (Hz)		
	Analysis		Test
	Original	After modifications	
First bending	37.5 (84 %)	41.5 (93 %)	44.4 (100 %)
First torsion	21.4 (75 %)	25.3 (89 %)	28.5 (100 %)

Table 5.3 Improvement of Results by Modifying the Connecting Beam Elements to Flexible Joints As Rigid Elements

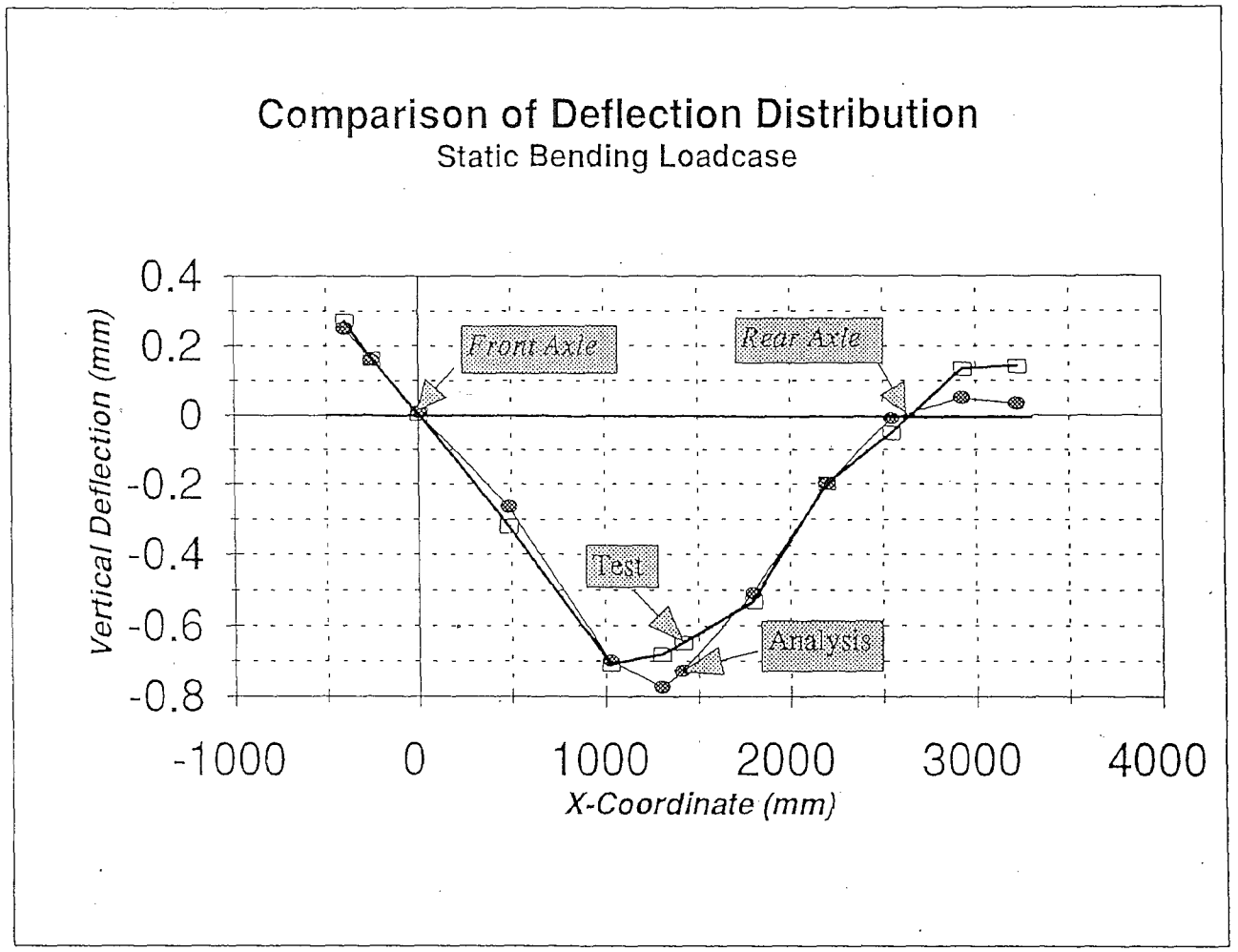

Figure 5.1 Comparison of Deflection Distributions for Static Bending Loadcase

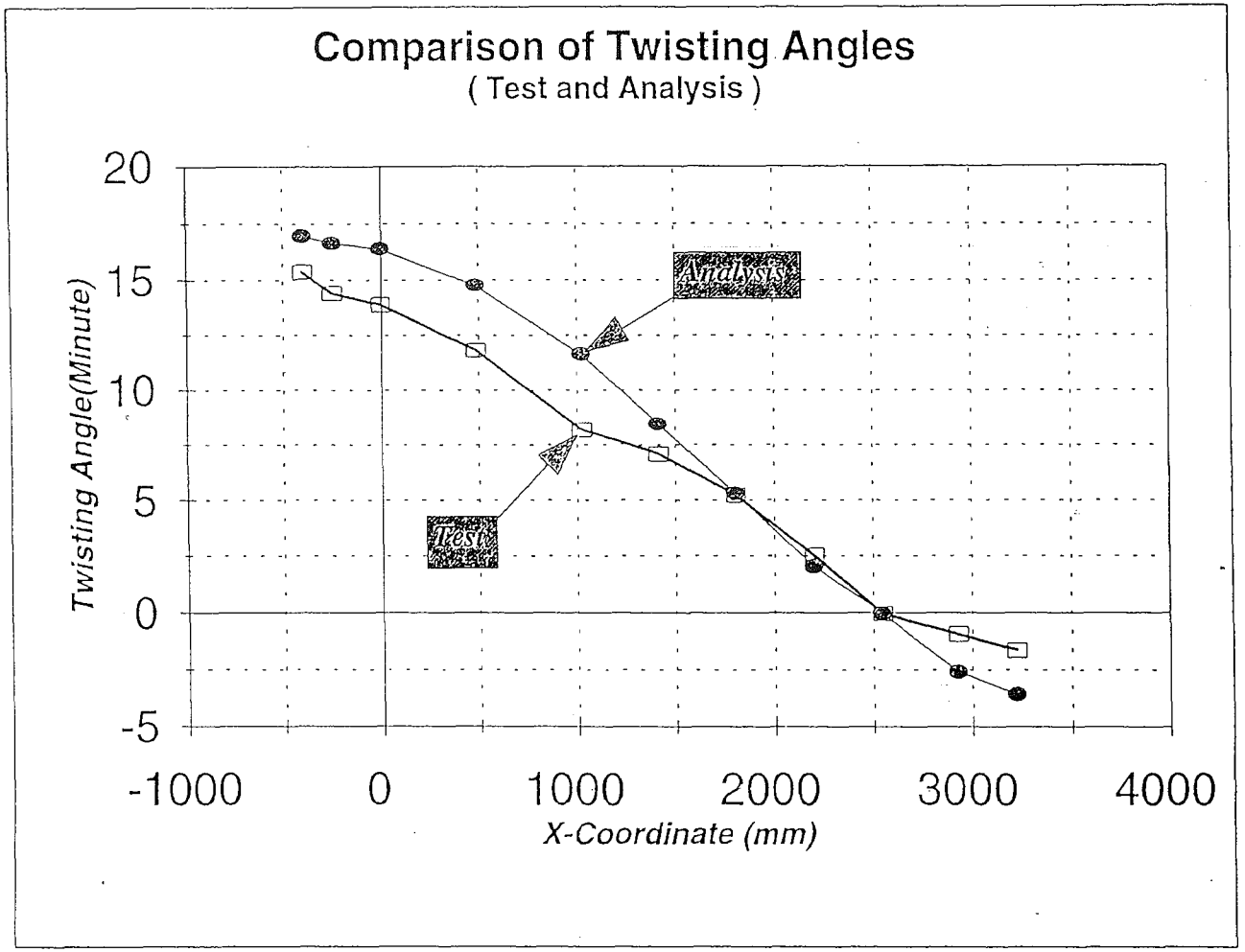

Figure 5.2 Comparison of Twisting Angle Distributions

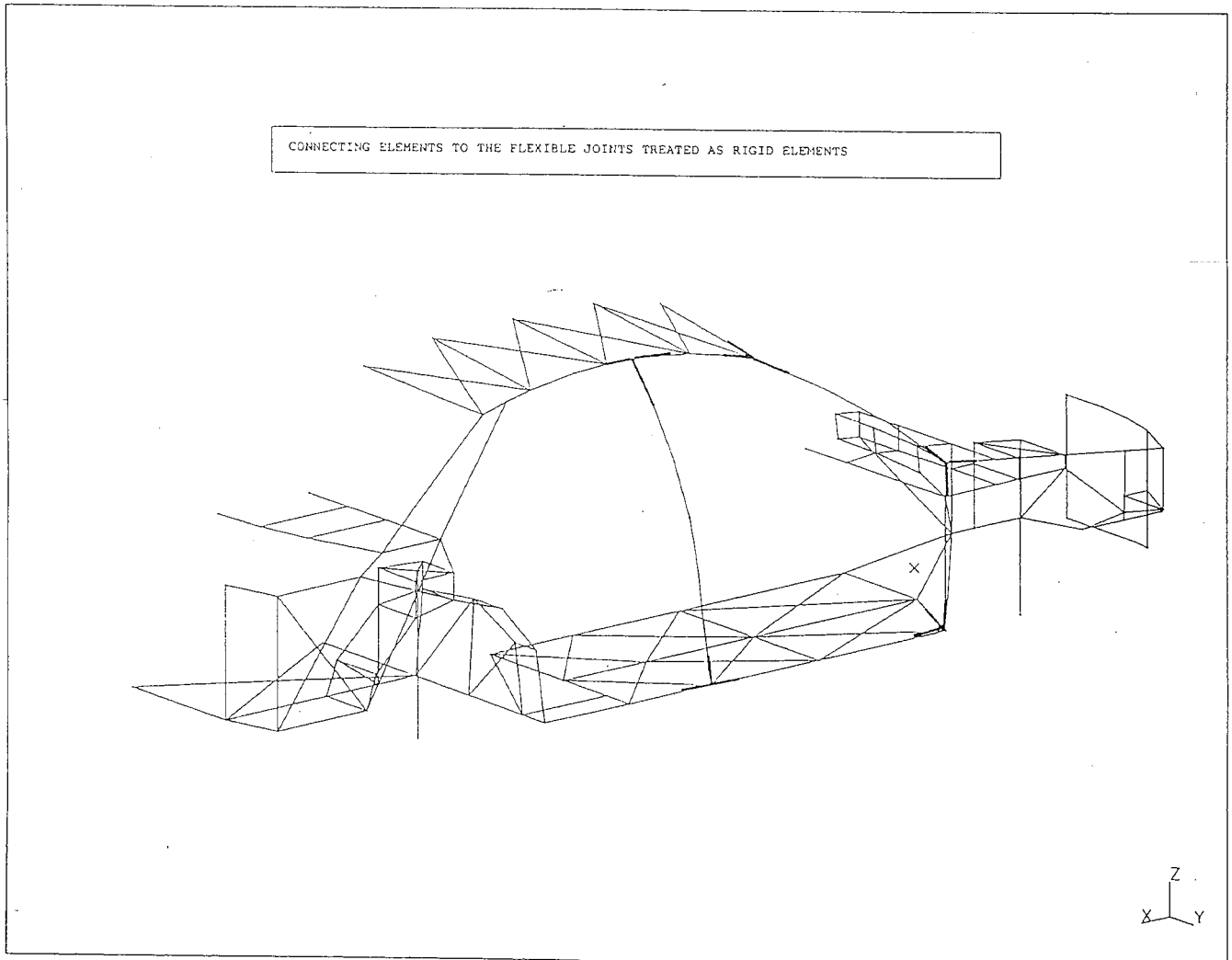

Figure 5.3 Connecting Beam Elements to Flexible Joints Treated as Rigid Elements

Chapter 6

CONCLUSIONS

Finite element analysis can evaluate the performance of the body structure for passenger cars, but a detailed model in the early stages of design is too complex and requires much computer time[25]. Furthermore, because it can be constructed only with detailed drawings, its execution may delay production and schedule.

In this thesis, a more simplified skeleton model which consists of beam elements has been developed to compensate for the problems of the detailed model[26]. According to the analyses of the skeleton model, the conclusions reached in this thesis were the following :

(1) The usefulness of skeleton model as a powerful analysis tool in body structure has been demonstrated and good agreement between analytic results and test results has been shown.

(2) Upon comparing those analytic results with test results obtained from Hyundai Motor Company, the percent error was 2.5 % for static bending stiffness, 16 % for static torsional rigidity, 7 % for first beaming frequency and 12 % for first torsional frequency respectively. The accuracy of these analytic results was more than 80 %.

(3) Highly complex structures can be reproduced with only a small number of beam elements, without sacrificing the accuracy of the main features of the solution, at a significant reduction in the cost of preparation and computation.

(4) The stiffness of the beam elements that surround the flexible joints must be increased, in comparison of the stiffness of the elements away from the joints. If the surrounding elements are made rigid, as shown in figure 5.3, then the results for the free vibration analysis are improved by about 10 %. From this result, it can be concluded that it is more reasonable and realistic to represent the surrounding beam elements of the flexible joints as rigid. But further work is needed in the future to decide exactly the length of beam elements which have to be represented as rigid elements.

(5) Bending results for static load cases as well as free vibration analysis are more accurate than those of torsional results. This is likely to be caused by insufficient representation of the inplane stretching effect for the panel parts in the skeleton model.

(6) If the analytic results of static and free vibration analysis are compared, it is seen that the results for static analysis are more precise than those of free vibration analysis. This may be attributed to the lack of representation of mass distribution for the body structure.

In spite of the need for some further work on the representation of the in-plane stretching effect and the mass distribution for the panel parts, the performance of the body structure can be predicted and evaluated easily by a well-correlated skeleton model, as the primary objectives of the design for the passenger cars, at the design concept stage, without any detailed drawings. Especially, it is possible to achieve the elimination of vibration problems of a full vehicle system, by avoiding the resonance

between the natural frequencies of the body structure and those of the engine, exhaust system etc., which are the sources of automobile vibration[27]. Furthermore, by using a skeleton model, a sensitivity analysis can be performed and eventually the optimization of the stiffness distribution in the body structure[28-29] can be pursued.

References

1. Kamal, M.M.,and Wolf, J.A., " Modern Automotive Structural Analysis," Van Nostrand Reinhold Company, New York, 1982.
2. "Structural Design and Crashworthiness of Automobile," T.K.S. Murthy and C.A. Brebbia, Computational Mechanics Publications, 1987.
3. Melosh, R.J., "Finite Element Analysis of Automobile Structures," in SAE Conference Proceedings, p 52.
4. " Vibration Problems in Engineering", Forth Edition, S. Timoshenko and D.H. Young and W. Weaver, JR., Stanford University.
5. "Analysis of Beam/Membrane Assemblies", D. Kecman, I. Kecman, V.Bulat, Yugoslavia, 1987.
6. S. Timoshenko, and S.Woinowsky-Krieger, " Theory of Plates and Shells," Second Edition, McGRAW-HILL, Inc, 1959.
7. Thomas J.R. Hughes, "The Finite Element Method",PRENTICE-HALL, Inc, 1987
8. C.S. DESAI, " Elementary Finite Element Method" , PRENTICE-HALL, Inc, 1979
9. " System Design with Substructures ", Cecil R. Rogers, Swanson Analysis System, Inc, 1977.
10. "International Conference on Vehicle Structural Mechanics: Finite Element Application to Vehicle Design", March 26-28, 1974, pp 26-38.
11. Nagy, L.I., "Static Analysis Via Substructuring of an Experimental Vehicle

Front-End Body Structure", 1974, pp 73-80.

12. Timoshenko and Goodier, "Theory of Elasticity", Third Edition, MaGRAW-HILL, Inc, 1970.
13. "Torsional Rigidity of a Racing Car Frame", J.R. Banerjee, Department of Aeronautics, The City University, Northamton Square, U.K., 1987.
14. James A. Augustitus, M. Kamal, and Larry J. Howell, " Design Through Analysis of an Experimental Automobile Structure", Research Labs, General Motors Corp,1977.
15. Wilkinson, J.H., "The Algebraic Eigenvalue Problem", Oxford University Press, 1965.
16. Bathe, K.J., "Finite Element Procedures in Engineering Analysis", Englewood Cliffs, Prentice-Hall, 1982.
17. " I-DEAS User's Manual", Structural Dynamics Research Corp, Ohio,1993.
18. Cook, Robert D., "Concepts and Applications of Finite Element Analysis",New York, John Wiley and Sons, Inc, 1981.
19. Guyan, R.J., "Reduction of Stiffness and Mass Matrices", AIAA Journal, Vol.3., No.2, 1965.
20. Cook, R., Malkus, D. and Plesha, M., "Concepts and Applications of Finite Element Analysis", Third Edition, New York, Wiley, 1989, pp 429-446.
21. Golub, G.H., Underwood, R., and Wilkinson,J.H., "The Lanczos Algorithm for the Symmetric Ax=Lambda*Bx Problem", Stanford University, Computer Science Department, 1972.

22. Theory of Vibration with Applications", William T. Thomson, Prentice-Hall, Inc, 1981.

23. Dowell, E.H., "Free Vibration of an Arbitrary Structure in Terms of Component Modes", ASME Journal of Applied Mechanics, Vol.39, 1972, pp 727-732.

24. Chang, D.C., " Effects of Flexible Connections on Body Structural Response," Automotive Engineering Congress, Detroit, Michigan, 1974, SAE No. 740041.

25. " Computational Methods in Ground Transportation Vehicles", M. Kamal and J.A. Wolf, JR., ASME, 1982.

26. "Application of Isoparametric Finite Elements in Vehicle Structural Mechanics", C.J. Parekh, J.E. Basas, and K.S. Kothawala, Engineering Mechanics Research Corp,1977.

27. Kamal, M.M., and Wolf, J.A., " Finite Element Applications in Vibration Problems," ASME, pp 67-92, New York, 1977.

28. "Experiences with Minimum Weight Design of Structures Using Optimality Criteria Methods", N.S. Khot, V.B. Venkayya, and L.Berke, Air Force Flight Dynamics Labs, 1978.

29. "Structural Optimization in Panel Design", David C. Chang and Martin R. Barone, Research Labs, General Motors Corp.,1977.

30. "MSC/NASTRAN User's Manual", MacNeal-Schwendler Corp., Los Angeles, California.

Appendix A. Typical Sections of the Body Structure in a Passenger Car

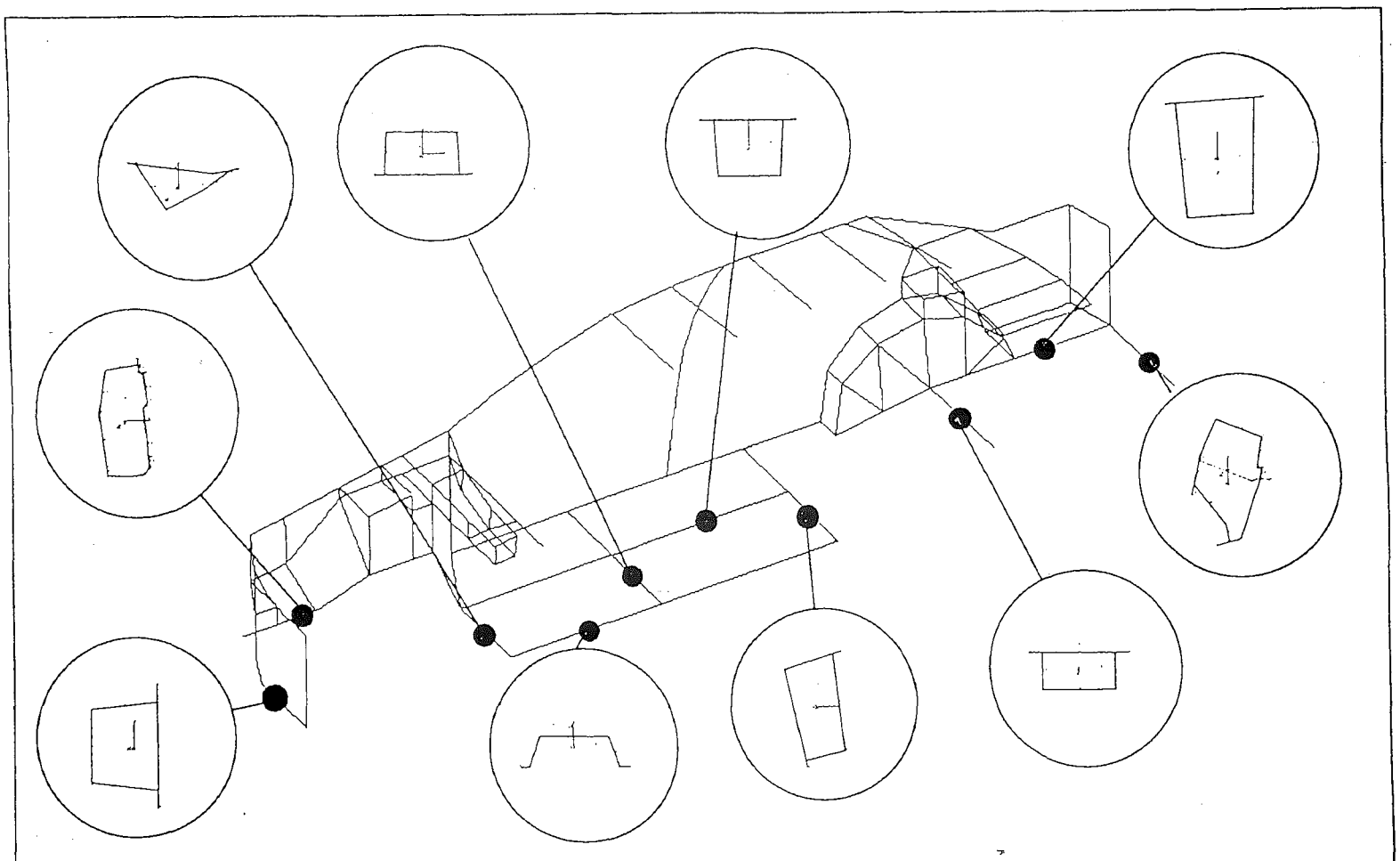

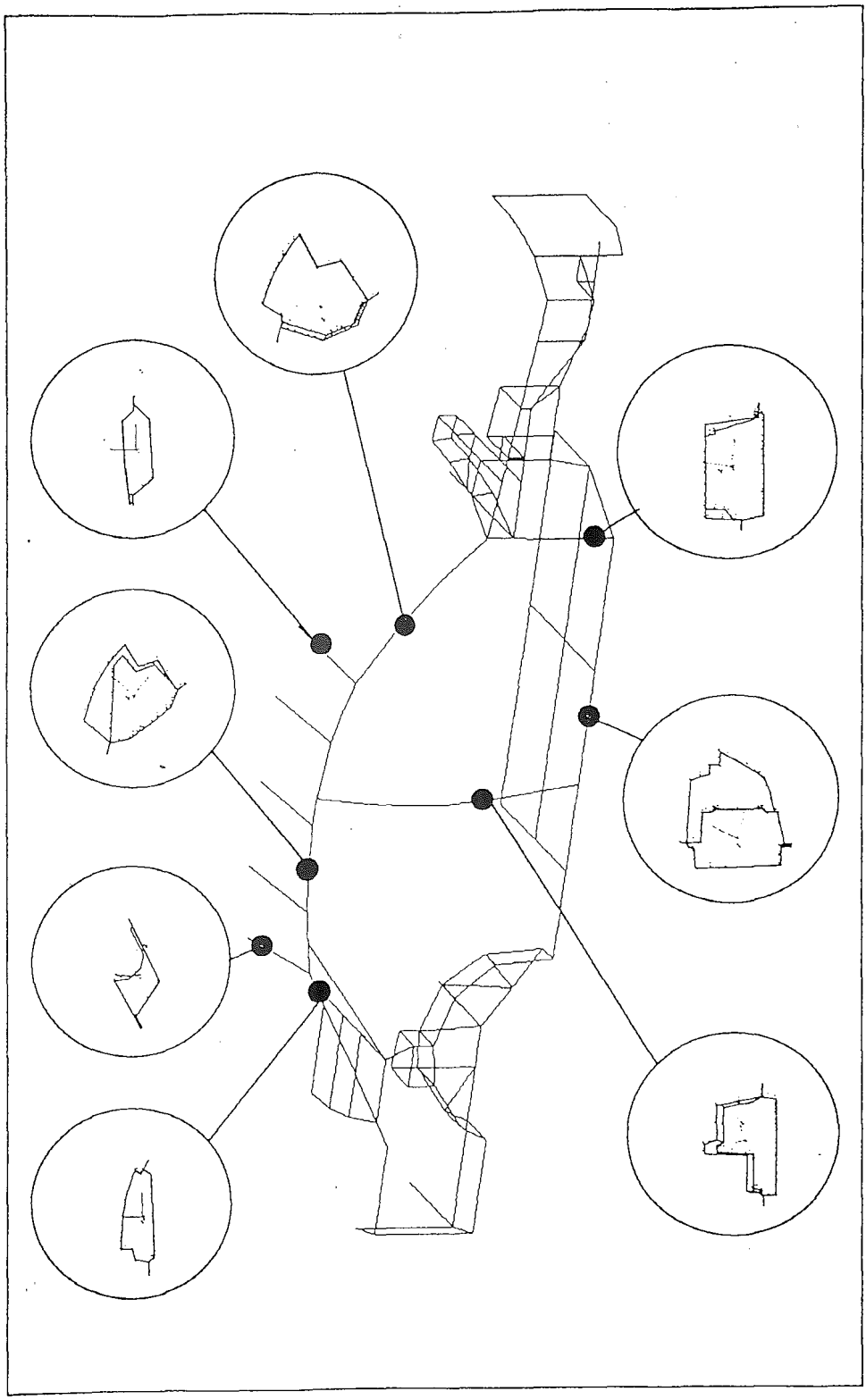

SIDE SILL FRAME

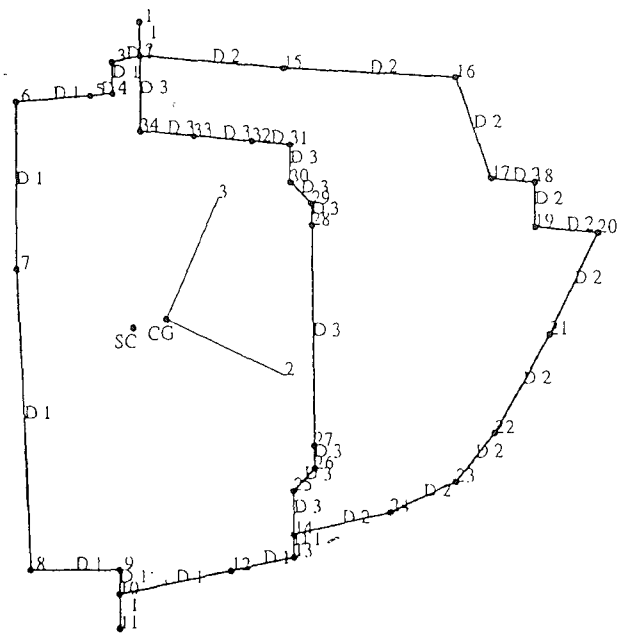

EQUATION OF PLANE

1.00 X +0.00 Y +0.00 Z = 5.93E+02

CENTER OF GRAVITY

593.00 662.61 33.69

AREA OF SECTION

8.16418E+02

3rd POINT ON 2-2 AXIS

0.00 91.02 -41.41

2nd MOMENTS OF INERTIA ABOUT C.G.

ABOUT 2-2 AXIS 1.55517E+06

ABOUT 3-3 AXIS 1.25208E+06

TORSIONAL CONSTANT 1.53595E+06

SHEAR CENTER TO C.G. IN L.C.S.

7.81 1.91

RADIATOR LOWER MEMBER

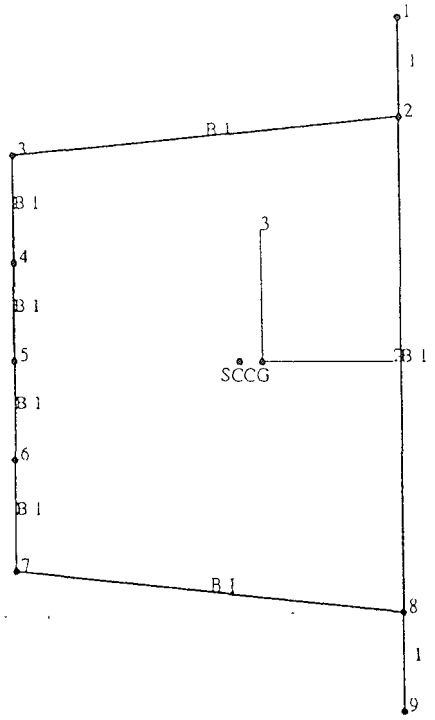

EQUATION OF PLANE

0.00 X -1.00 Y +0.00 Z = 0.00E+00

CENTER OF GRAVITY

-502.35 0.00 327.50

AREA OF SECTION

9.19596E+01

3rd POINT ON 2-2 AXIS

100.00 0.00 0.00

2nd MOMENTS OF INERTIA ABOUT C.G.

ABOUT 2-2 AXIS 1.02708E+04

ABOUT 3-3 AXIS 6.30553E+03

TORSIONAL CONSTANT 8.33897E+03

SHEAR CENTER TO C.G. IN L.C.S.

1.19 0.00

FRONT SIDE MEMBER

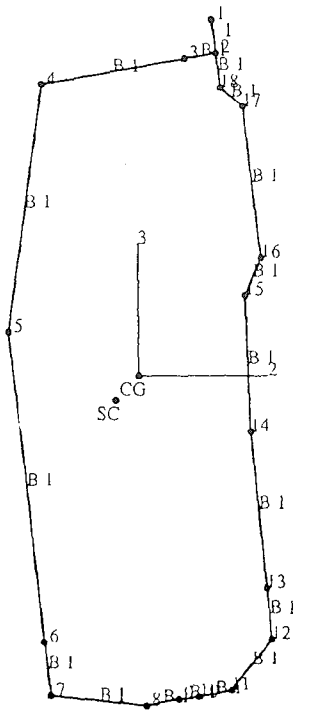

EQUATION OF PLANE

1.00 X +0.00 Y +0.00 Z = 1.17E+02

CENTER OF GRAVITY

117.00 452.58 273.37

AREA OF SECTION

5.41515E+02

3rd POINT ON 2-2 AXIS

0.00 99.37 -11.20

2nd MOMENTS OF INERTIA ABOUT C.G.

ABOUT 2-2 AXIS	1.54499E+06
ABOUT 3-3 AXIS	3.35605E+05

TORSIONAL CONSTANT 8.79008E+05

SHEAR CENTER TO C.G. IN L.C.S.

5.89 5.81

DASH LOWER MEMBER

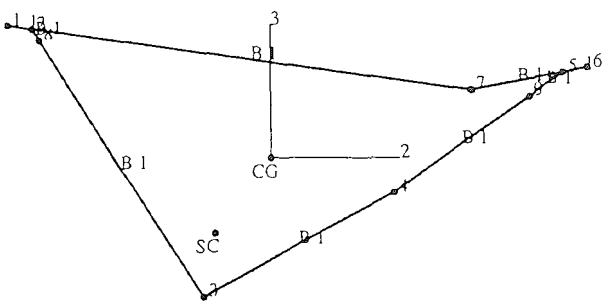

EQUATION OF PLANE

0.00 X -1.00 Y +0.00 Z = 2.70E+02

CENTER OF GRAVITY

273.36 270.00 28.68

AREA OF SECTION

8.56397E+02

3rd POINT ON 2-2 AXIS

83.46 0.00 -55.09

2nd MOMENTS OF INERTIA ABOUT C.G.

ABOUT 2-2 AXIS	5.28766E+05
ABOUT 3-3 AXIS	2.18844E+06

TORSIONAL CONSTANT 5.67012E+05

SHEAR CENTER TO C.G. IN L.C.S.

18.18 23.73

CENTER FLOOR SIDE MEMBER

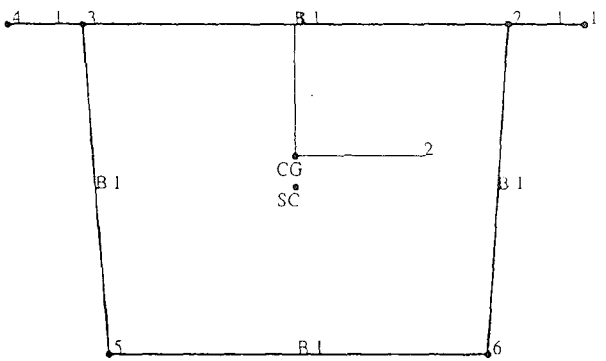

EQUATION OF PLANE

1.00 X +0.00 Y +0.00 Z = 0.00E+00

CENTER OF GRAVITY

0.00 313.00 51.40

AREA OF SECTION

1.29629E+02

3rd POINT ON 2-2 AXIS

0.00 100.00 0.00

2nd MOMENTS OF INERTIA ABOUT C.G.

ABOUT 2-2 AXIS 2.67714E+04

ABOUT 3-3 AXIS 4.64761E+04

TORSIONAL CONSTANT 3.81664E+04

SHEAR CENTER TO C.G. IN L.C.S.

0.00 3.15

CENTER FLOOR TUNNEL

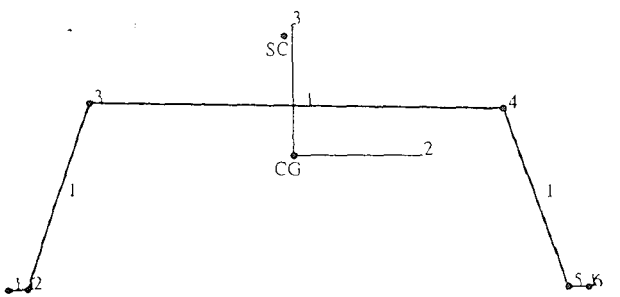

EQUATION OF PLANE

1.00 X +0.00 Y +0.00 Z = 8.11E+02

CENTER OF GRAVITY

811.00 -0.69 50.32

AREA OF SECTION

2.95551E+02

3rd POINT ON 2-2 AXIS

0.00 100.00 -0.60

2nd MOMENTS OF INERTIA ABOUT C.G.

ABOUT 2-2 AXIS 2.95384E+05

ABOUT 3-3 AXIS 2.82890E+06

TORSIONAL CONSTANT 4.82733E+01

SHEAR CENTER TO C.G. IN L.C.S.

4.02 -59.59

FRONT SEAT CROSS MEMBER

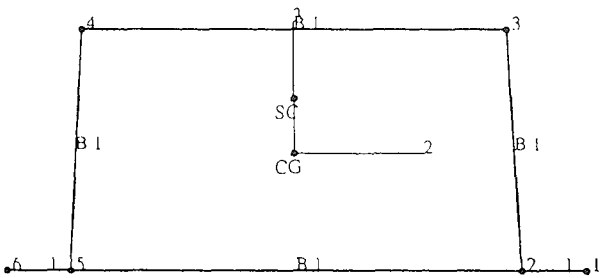

EQUATION OF PLANE

0.00 X -1.00 Y +0.00 Z = 0.00E+00

CENTER OF GRAVITY

877.00 0.00 214.91

AREA OF SECTION

2.03765E+02

3rd POINT ON 2-2 AXIS

100.00 0.00 0.00

2nd MOMENTS OF INERTIA ABOUT C.G.

ABOUT 2-2 AXIS 3.36163E+04

ABOUT 3-3 AXIS 1.09231E+05

TORSIONAL CONSTANT 5.90521E+04

SHEAR CENTER TO C.G. IN L.C.S.

0.00 -6.61

REAR FLOOR SIDE MEMBER

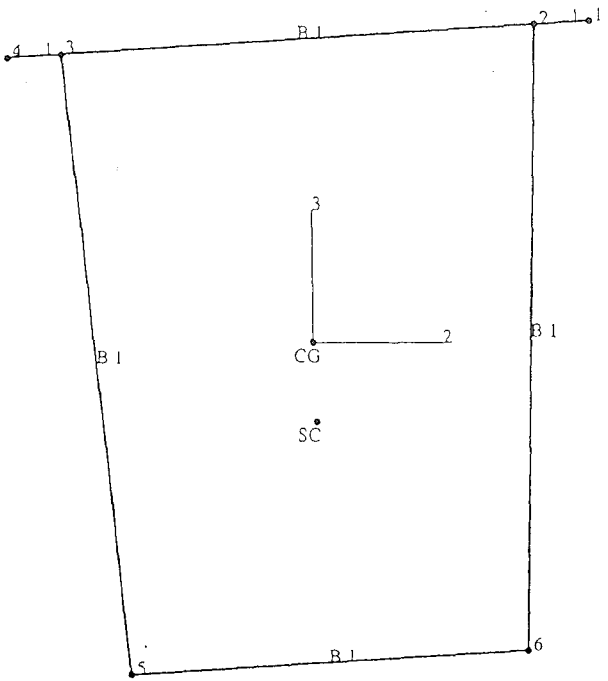

EQUATION OF PLANE

1.00 X +0.00 Y +0.00 Z = 0.00E+00

CENTER OF GRAVITY

0.00 460.87 291.63

AREA OF SECTION

3.62956E+02

3rd POINT ON 2-2 AXIS

0.00 99.81 -6.10

2nd MOMENTS OF INERTIA ABOUT C.G.

ABOUT 2-2 AXIS	4.36172E+05
ABOUT 3-3 AXIS	3.03509E+05

TORSIONAL CONSTANT 4.35733E+05

SHEAR CENTER TO C.G. IN L.C.S.

-0.42 11.39

REAR FLOOR FRONT EXTENSION

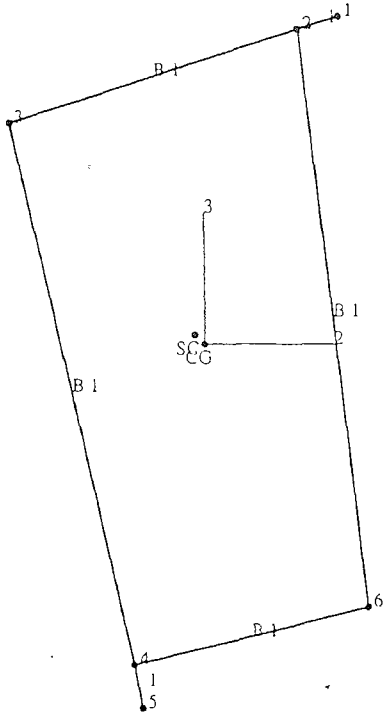

EQUATION OF PLANE

0.00 X -1.00 Y +0.00 Z = 0.00E+00

CENTER OF GRAVITY

1653.52 0.00 285.39

AREA OF SECTION

2.39012E+02

3rd POINT ON 2-2 AXIS

95.43 0.00 -29.89

2nd MOMENTS OF INERTIA ABOUT C.G.

ABOUT 2-2 AXIS	4.01629E+05
ABOUT 3-3 AXIS	1.18998E+05

TORSIONAL CONSTANT 2.49355E+05

SHEAR CENTER TO C.G. IN L.C.S.

1.78 -1.71

REAR FLOOR CENTER CROSS MEMBER

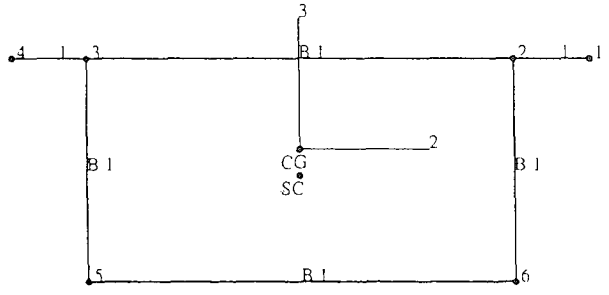

EQUATION OF PLANE

0.00 X -1.00 Y +0.00 Z = 0.00E+00

CENTER OF GRAVITY

2474.00 0.00 151.69

AREA OF SECTION

1.17600E+02

3rd POINT ON 2-2 AXIS

100.00 0.00 0.00

2nd MOMENTS OF INERTIA ABOUT C.G.

ABOUT 2-2 AXIS 1.21494E+04

ABOUT 3-3 AXIS 4.27824E+04

TORSIONAL CONSTANT 2.20546E+04

SHEAR CENTER TO C.G. IN L.C.S.

0.00 2.68

ROOF FRONT RAIL

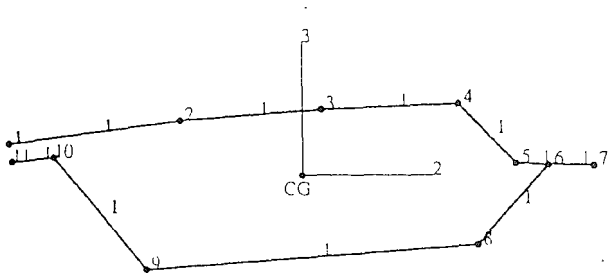

SC

EQUATION OF PLANE

0.00 X +1.00 Y +0.00 Z = 0.00E+00

CENTER OF GRAVITY

764.43 0.00 1320.65

AREA OF SECTION

1.48463E+02

3rd POINT ON 2-2 AXIS

-87.51 0.00 -48.40

2nd MOMENTS OF INERTIA ABOUT C.G.

ABOUT 2-2 AXIS 1.52059E+04

ABOUT 3-3 AXIS 1.40297E+05

TORSIONAL CONSTANT 2.55400E+01

SHEAR CENTER TO C.G. IN L.C.S.

-77.09 4.24

ROOF SIDE RAIL

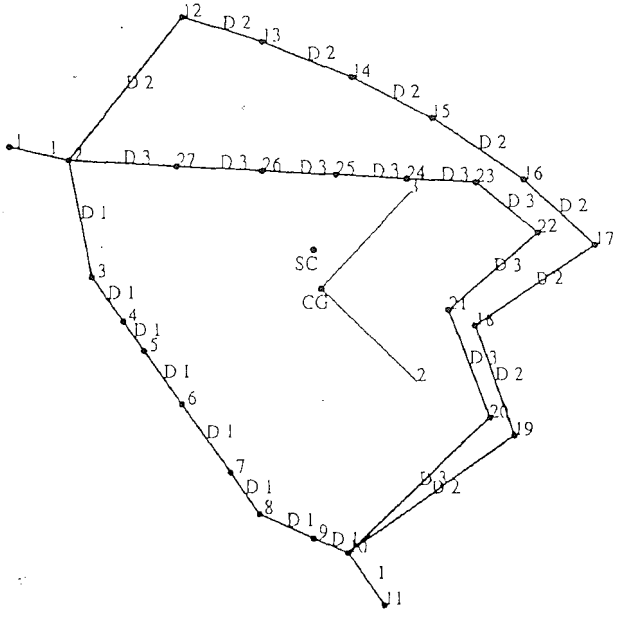

EQUATION OF PLANE

1.00 X +0.00 Y +0.00 Z = 1.28E+03

CENTER OF GRAVITY

1280.00 489.69 1075.52

AREA OF SECTION

2.84319E+02

3rd POINT ON 2-2 AXIS

0.00 72.31 -69.07

2nd MOMENTS OF INERTIA ABOUT C.G.

ABOUT 2-2 AXIS 8.84999E+04

ABOUT 3-3 AXIS 1.60463E+05

TORSIONAL CONSTANT 1.28494E+05

SHEAR CENTER TO C.G. IN L.C.S.

0.92 -4.97

ROOF REAR RAIL

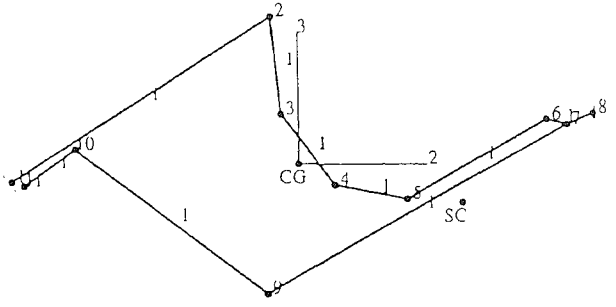

EQUATION OF PLANE

0.00 X -1.00 Y +0.00 Z = 0.00E+00

CENTER OF GRAVITY

2487.61 0.00 1344.49

AREA OF SECTION

2.93198E+02

3rd POINT ON 2-2 AXIS

78.65 0.00 -61.75

2nd MOMENTS OF INERTIA ABOUT C.G.

ABOUT 2-2 AXIS	8.67496E+04
ABOUT 3-3 AXIS	5.56043E+05

TORSIONAL CONSTANT 6.17063E+01

SHEAR CENTER TO C.G. IN L.C.S.

-44.42 10.19

FRONT PILLAR UPPER

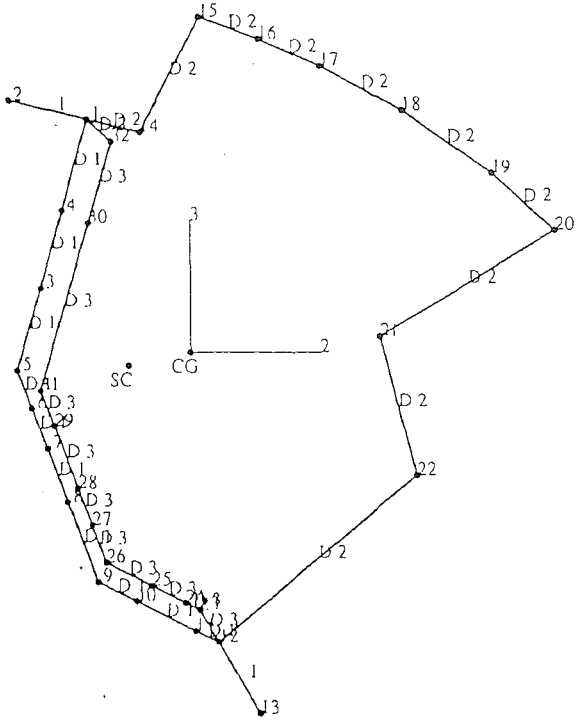

EQUATION OF PLANE

0.85 X -0.26 Y +0.45 Z = 1.13E+03

CENTER OF GRAVITY

977.39 546.28 980.36

AREA OF SECTION

2.33101E+02

3rd POINT ON 2-2 AXIS

26.44 96.24 6.18

2nd MOMENTS OF INERTIA ABOUT C.G.

ABOUT 2-2 AXIS 9.46141E+04

ABOUT 3-3 AXIS 5.28015E+04

TORSIONAL CONSTANT 6.50010E+04

SHEAR CENTER TO C.G. IN L.C.S.

6.27 1.28

FRONT PILLAR LOWER

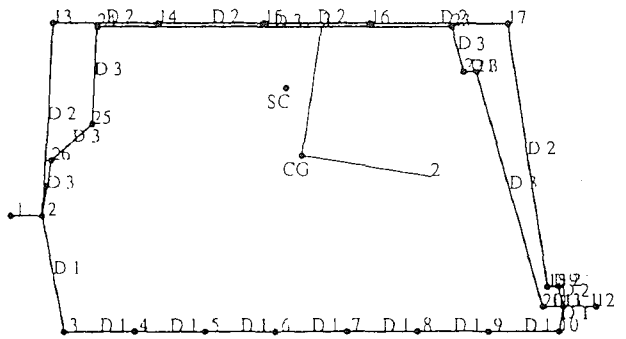

EQUATION OF PLANE

0.00 X +0.00 Y +1.00 Z = 3.30E+02

CENTER OF GRAVITY

456.47 692.56 330.00

AREA OF SECTION

5.91873E+02

3rd POINT ON 2-2 AXIS

98.73 -15.90 0.00

2nd MOMENTS OF INERTIA ABOUT C.G.

ABOUT 2-2 AXIS	4.90681E+05
ABOUT 3-3 AXIS	1.33204E+06

TORSIONAL CONSTANT 8.97287E+05

SHEAR CENTER TO C.G. IN L.C.S.

3.79 -16.50

CENTER PILLAR LOWER

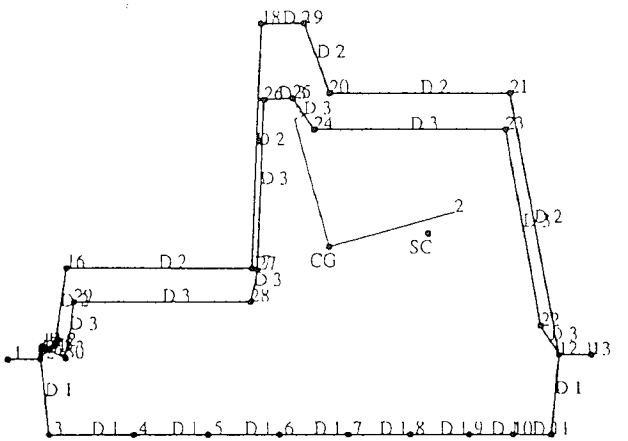

EQUATION OF PLANE

0.00 X +0.00 Y +1.00 Z = 3.50E+02

CENTER OF GRAVITY

1430.57 694.62 350.00

AREA OF SECTION

9.15019E+02

3rd POINT ON 2-2 AXIS

96.65 25.67 0.00

2nd MOMENTS OF INERTIA ABOUT C.G.

ABOUT 2-2 AXIS	6.62667E+05
ABOUT 3-3 AXIS	1.56286E+06

TORSIONAL CONSTANT 7.81061E+05

SHEAR CENTER TO C.G. IN L.C.S.

-24.27 -3.17

QUARTER PILLAR UPPER

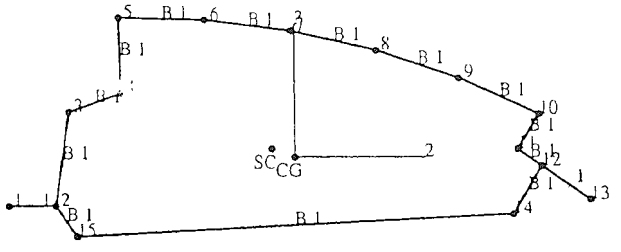

EQUATION OF PLANE

-0.75 X -0.33 Y +0.58 Z = 1410.525

CENTER OF GRAVITY

2340.50 579.92 924.20

AREA OF SECTION

3.35487E+02

3rd POINT ON 2-2 AXIS

66.27 -34.21 66.62

2nd MOMENTS OF INERTIA ABOUT C.G.

ABOUT 2-2 AXIS	1.41174E+05
ABOUT 3-3 AXIS	8.17920E+05

TORSIONAL CONSTANT 3.24908E+05

SHEAR CENTER TO C.G. IN L.C.S.

6.28 -2.24

BACK PANEL & TRANSVERSE

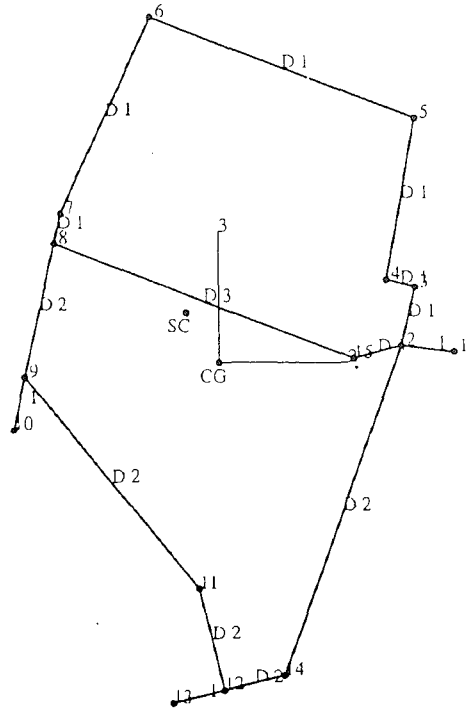

EQUATION OF PLANE

0.00 X -1.00 Y +0.00 Z = 0.00E+00

CENTER OF GRAVITY

2712.89 0.00 326.72

AREA OF SECTION

2.89704E+02

3rd POINT ON 2-2 AXIS

93.70 0.00 34.94

2nd MOMENTS OF INERTIA ABOUT C.G.

ABOUT 2-2 AXIS	2.03830E+05
ABOUT 3-3 AXIS	1.15803E+05

TORSIONAL CONSTANT 1.21876E+02

SHEAR CENTER TO C.G. IN L.C.S.

4.96 -7.41

Vita

Jun. 16, 1960	Born in Masan, Korea
Feb.24, 1986	B.S., Yonsei University Seoul, Korea
Jan.4, 1986- Aug.1,1994	Design Engineer, Hyundai Motor Company
Aug. 1994- Jun. 1996	Graduate Student, Lehigh University Supported by Hyundai Motor Company
Aug. 1996-	Design Engineer, Hyundai Motor Company

END OF TITLE